Cognitive impairment in neurodegenerative diseases:

insights from computational neuroimaging

Alexander V Lebedev MD

Dissertation for the degree philosophiae doctor (PhD)

at the University of Bergen

2014

For my Grandparents, Nikolai and Nadezhda Lebedevs

Table of contents

Scientific environment

Centre for Age-Related Medicine

Stavanger University Hospital

Stavanger, Norway

Department of Clinical Medicine

University of Bergen

Bergen, Norway

Overview

The project has been conducted at the Centre for age-related medicine (Regionalt kompetansesenter for eldremedisin og samhandling, SESAM) at the Stavanger University hospital (SUS) under the supervision given by Prof. Dag Aarsland MD PhD, who is research director of SESAM, professor of clinical dementia research at Alzheimer's Disease Research Centre, NVS, Karolinska Institutet, and principal investigator of the DemWest study group.

Alexander Lebedev MD is a medical doctor (specialized in psychiatry), with experience in multimodal neuroimaging (PET, fMRI, anatomical MRI, DTI, MRS). He participated in imaging studies of depression and anxiety disorders, performing analysis of structural and functional imaging data. He is also familiar with modern approaches to multivariate data analysis and machine learning

techniques. He has been employed as a researcher at SESAM since 2011, and was a PhD student in this project.

Co-supervision was given by:

Prof. Nils Erik Gilhus MD PhD, who is the head of the Department of Clinical Medicine (University of Bergen). He coordinated the project, guiding and assessing the study progress, provided overall clinical and academic supervision and expertise;

Eric Westman PhD is an assistant professor at the Department of Neurobiology, Care Sciences and Society (Karolinska Institute, Stockholm, Sweden), experienced in neuroscience, neuroimaging, advanced approaches to multivariate data analysis and machine learning algorithms. He coordinated the imaging part of the project, helped with practical support and critical review of the papers;

Mona Beyer MD PhD is a neuroradiologist at Oslo University Hospital, MRI coordinator of the DemWest study and recently worked as a post doc researcher with support from the Western Norway regional health authority. She helped with practical support, critical review of the papers and provided imaging expertise to the project;

Prof. Arvid Lundervold MD PhD, who is a professor at the Department of Biomedicine (University of Bergen) and the head of the Neuroinformatics and Image Analysis Laboratory (a part of the Neuroscience Research group). He provided expert imaging and numerical input to the project, helped with critical review of the manuscripts.

Other collaborators:

Prof. Clive Ballard MD PhD (King's College London, UK) is a world-leading dementia researcher, visiting professor at SESAM and expert consultant for the DemWest project. He provided clinical and research expertise to the project.

Gerard JP Van Westen PhD is a post doc researcher at the European Bioinformatics Institute (EMBL-EBI, Hinxton, Cambridgeshire, UK) with expertise in machine learning and computer-aided drug discovery. He provided technical input to the project, specifically concerning implementation of the Random Forest algorithm for imaging data, and was included as a co-author in the paper II.

Milica Kramberger MD is a neurologist and the head of at the University Medical Centre for cognitive disorders in Ljubljana (Slovenia). She is a research coordinator in Slovenian dementia study and our collaborator with expertise in functional and structural imaging data analysis. Imaging data from their study, provided by her research group, have been included in the papers I and II.

Andy Simmons PhD is a Consultant Clinical Scientist (Medical Physics) at the South London and Maudsley NHS Foundation Trust and a lecturer at the Department of Neuroimaging, Institute of Psychiatry, King's College London and the NIHR Biomedical Research Centre for Mental Health. He is also a member of the AddNeuroMed Consortium, responsible for the image protocol harmonization, acquisition and analysis. He provided access to the AddNeuroMed cohort, participated in the data analysis, provided technical input and critical review of the papers II and IV.

Acknowledgements

There are several people without whom this project would never be accomplished. If you asked me who was the key person in this project I would certainly highlight my main supervisor Dag Aarsland. Of course, everyone should write good words about his/her boss, but in my case this is an extremely easy task. I still do not know where he finds time, energy and patience to guide all his students so effectively and at the same time managing several international research projects! Dag is also the one who introduced me to the high quality medical research, teaching me how to plan, design, and perform studies, how to implement, report and defend your ideas. As I am writing this thesis, my clinical career in Europe has not started yet, but observing Dr. Aarsland in action, during patient interviews, I already see what a great clinician he is and hope to keep learning from him.

I am also very grateful to Eric Westman, my second supervisor from Karolinska who supported my ideas and helped a lot with his imaging and numerical expertise. Specifically, I want to thank him for his constructive criticism and very friendly attitude in all stages of this project.

Mona K. Beyer deserves a very special acknowledgement. Being a person who taught me how to plan, conduct research and how to write papers, she was also the one who knew what I needed when I first came to Stavanger, sometimes even better than I did. I will never forget our talk at the Gardermoen airport, all your suggestions and inspirations!

I would like to acknowledge Dr. Nils Erik Gilhus for his highly valuable practical support and contribution. Thanks to him, my project was running very effectively and all the components had been completed just in time.

I met Dr. Arvid Lundervold during my first visit in Bergen in 2011. His presentation was one of the most important reasons why I decided to start my PhD at the University of Bergen. It was astonishing! And after a while I was

happy to have him as a co-supervisor, who helped with his wide-ranging expertise and provided access to the UiB supercomputers. This allowed me to work at the very high speeds I have never experienced before.

Finally, I want to thank all my supervisors for their patience, when tolerating my stubbornness and helping me with very constructive and at the same time still very positive and friendly recommendations and feedback. I am fully aware of how annoying I may become if I disagree with something.

Françoise J. Siepel is my dearest colleague in Stavanger and also my closest Norwegian friend! I already miss our talks and I am very grateful for all your support and help.

Many thanks to Ingelin Testad, our "two dear Kristins" (Kristin Nordin and Kristin Lexow), Helen Wigestrand, who created bright atmosphere at SESAM and without whom I would probably not be able to make a single step in my research career, just being puzzled with my paperwork.

Dr. Jan Olav Johannessen, Karin Smedvig, Viktoria Weggeberg are those thanks to whom I got a chance to come to Norway and started my academic career. Thank you for all your support!

My Russian Teachers and Colleagues… Arkadiy Korzenev, who once literally saved my professional and research life (you know what I mean, Arkadiy Vladimirovich). He, Eugeniy Abritalin, Vladimir Fokin, Degtyarenko Vyacheslav are my first Teachers and I am extremely grateful for everything that you have done for me, for opening the doors of science. Dmitriy Tarumov, Alexander Efimtcev, Andrey Sevastyanov, Andrey Sokolov – working with you in Russia was a fantastic experience for me, and we should definitely stay in touch!

It is almost impossible to exaggerate how much each member of my family has contributed to my work…. My wife Alexandra, who I love and respect not only as a person and a woman, but also as an attentive doctor and a very bright

scientist. She did and does play a crucial role in my work; every idea, every analysis, every result - everything has been discussed with her and/or commented by her. My mother, Olga Lebedeva also played a very important role. Even after all these years of living far from Home, I always feel your presence, love and support. I am sure that you know how important you are to me!

Finally, one should never forget that all the studies and projects that we managed to accomplish or initiate became possible mainly thanks to the patients and their families who volunteered to participate. Thank you very much for all your contributions. You are truly the main characters in this work!

Abstract

Background

Cognitive impairment is a very common problem, especially in older individuals with major impact on quality of life, daily functioning, and healthcare. Its importance is expected to increase due to the demographic changes. Neuroimaging is a rapidly developing field of neuroscience that provides an opportunity to study brain mechanisms of cognitive impairment in vivo, which may help in the development of new biomarkers and treatment strategies. The application of advanced image processing to neuroimaging offers the potential for diagnostically relevant analysis techniques, in particular for magnetic resonance imaging (MRI).

Aim

The primary aims of the project were to investigate brain mechanisms of cognitive impairment in neurodegenerative diseases using computational neuroimaging approaches and to assess their potential applicability in clinical practice for detection, prediction and differential diagnosis of cognitive impairment in the elderly.

Objectives

1) To investigate brain changes underlying cognitive impairment in neurodegenerative diseases (Alzheimer's, Lewy body dementia and Parkinson's disease).
2) To assess the applicability of pattern recognition techniques for:
   a) Differential diagnosis of cognitive impairment

b) Prediction of further cognitive deterioration in patients with mild cognitive impairment;

3) To investigate problems associated with implementation of computer-aided image-based tools for detection, prediction and differential diagnosis of cognitive impairment.

Methods

Five datasets of clinical and imaging data were used, including two large-scale databases of Alzheimer's disease (ADNI and AddNeuroMed).

In the papers I-II, Alzheimer's disease was diagnosed according to the NINCDS-ADRDA criteria.

Dementia with Lewy bodies (paper I) was diagnosed according to the revised consensus criteria (1)

Image post-processing steps were performed within the surface- (papers I-III) and voxel-based (paper IV) frameworks using the Freesurfer and SPM8, respectively. Mass-univariate (papers III, IV) and multivariate (papers I, II and IV) approaches were used. In the paper IV, an automated quantitative meta-analysis was also performed using the Neurosynth software.

Results

Papers I-II

Optimizing image preprocessing and data analysis pipeline, we found that it is possible to develop a computer-aided tool for detection (Sensitivity/Specificity = 88.6%/92.0%), prediction (Sensitivity/Specificity = 83.3%/81.3%) and differential diagnosis (AD/DLB overall classification accuracy = 83.9%) of degenerative diseases with good between-cohort robustness if imaging and clinical protocols are carefully aligned. For the morphometric data, the use of disease-specific brain parcellation schemes resulted in equivalent performance

compared to normalized raw high-dimensional input, but required substantially lesser tuning time and computation/memory resources. Better accuracy of the models can be achieved by adding more biomarkers (e.g., ApoE genotype), demographics, and improved disease verification strategies (e.g., post-mortem diagnosis) for the data used as a training material for the classifiers.

The next two papers were focused on neural correlates of cognitive impairment in PD that had to be investigated prior considering them within the framework of computer-aided diagnosis.

Papers III-IV

We found that Parkinson's-related cognitive impairment affecting multiple domains is associated with temporo-parietal and superior frontal thinning. On a large-scale network level, better executive performance in PD is associated with increased dorsal fronto-parietal cortical processing and inhibited subcortical and primary sensory involvement when the subject is at resting state. This pattern is positively influenced by the relative preservation of nigrostriatal dopaminergic function. The pattern associated with better memory performance favors prefronto-limbic processing, and does not reveal associations with presynaptic striatal dopamine function.

Conclusions

Cognitive impairment in the elderly has different brain profiles depending on the predominant neurodegenerative pathology and cognitive functions affected. With the use of automated computer-aided tools and advanced image processing techniques, Alzheimer's disease can be robustly identified, predicted two years before the actual dementia onset and differentiated from dementia with Lewy bodies. After certain modifications and adaptations for clinicians, the models can be successfully incorporated into medical decision-support systems and be evaluated in subsequent diagnostic clinical trials.

The identified brain structural and functional profile associated with Parkinson's-related cognitive impairment is also robust and, holding strong diagnostic potential, must be detectable using computer-aided systems of similar design, the development of which is the matter of our future research. The development and future elaboration of clinically realistic computer-aided systems for the diagnosis of neurodegenerative diseases is an important topic for future research.

List of abbreviations

3D -Three dimensional

AD - Alzheimer's disease

ADNI - Alzheimer's Disease Neuroimaging Initiative

CAD - Computer-Aided Diagnosis

ChAT - Choline Acetyltransferase

CSF - Cerebrospinal fluid

CT - Computed tomography

DAT - Dopamine Transporter

DLB - Dementia with Lewy Bodies

DSM-IV - Diagnostic and Statistical Manual of Mental Disorders, version IV

ECG - Electrocardiogram

FFE - Fast Field Echo

FLAIR - Fluid Attenuation Inversion Recovery

FP-CIT - Iodine I 123-radiolabeled 2beta-carbomethoxy-3beta-(4-iodophenyl)-N-(3-fluoropropyl) nortropane

FSPGR - Fast spoiled gradient recalled echo

FWE - Family-Wise Error

FWHM - Full Width at Half Maximum

ICV - intracranial volume

LB - Lewy bodies

LBD - Lewy Body Dementia (DLB and PDD)

LV - Latent Variable

mAChRs - muscarinic acetylcholine receptors

MADRS - Montgomery Asberg Depression Rating Scale

MCI - Mild Cognitive Impairment

MCT - Mean Cortical Thickness

MDS - Movement Disorder Society

MIBG - Metaiodobenzylguanidine

MMSE - Mini mental state examination

MRI - Magnetic resonance imaging

NINCDS-ADRDA - National Institute of Neurological and Communicative Disorders and Stroke and the Alzheimer's Disease and Related Diseases Association

NPI - The Neuropsychiatric Inventory

PCA - Principal Component Analysis

PD - Parkinson's Disease

PDD - Parkinson's disease with dementia

PLS - Partial Least Squares

PPMI - Parkinson's Progression Markers Initiative

QOL - Quality Of Life

rCBF - regional Cerbral Blood Flow

RF - Random Forest

RFE - Recursive Feature Elimination

SPECT - Single-Photon Emission Computed Tomography

SPLS - Sparse Partial Least Squares

SPM - Statistical Parametric Mapping

SVM - Support Vector Machine

TE - Echo Time

TI - Inversion Time

TR - Repetition Time

UPDRS - Unified Parkinson’s Disease Rating Scale

VBM - Voxel-Based Morphometry

List of publications

1. Lebedev AV, Westman E, Beyer MK, Kramberger MG, Aguilar C, Pirtosek Z, Aarsland D. Multivariate classification of patients with Alzheimer's and dementia with Lewy bodies using high-dimensional cortical thickness measurements: an MRI surface-based morphometric study. Journal of Neurology, 2013. 260:1104-1115. DOI: 10.1007/s00415-012-6768-z

2. Lebedev AV, Westman E, Van Westen GJP, Aarsland D, Lundervold A, Simmons A. Random Forest ensembles for detection and prediction of Alzheimer's Disease with a good between-cohort robustness (Submitted);

3. Pereira JB, Svenningsson P, Weintraub D, Brønnick K, Lebedev A, Westman E, Aarsland D, Progression Markers Initiative. Initial cognitive decline is associated with cortical thinning in early Parkinson's disease. Neurology, 2014 (Accepted for publication in Neurology, 2014);

4. Lebedev AV, Westman E, Simmons A, Lebedeva A, Siepel FJ, Pereira JB and Aarsland D. Large-scale resting state network correlates of cognitive impairment in Parkinson's disease and related dopaminergic deficits. Frontiers in Systems Neuroscience, 2014. DOI: 10.3389/fnsys.2014.00045

Other publications

1. Siepel FJ, Brønnick KS, Booij J, Ravina BM, Lebedev AV, Pereira JB, Grüner R, Aarsland D. Cognitive executive impairment and dopaminergic deficits in de-novo Parkinson's disease: an [123I]FP-CIT SPECT study (Submitted);

2. Nouretdinov I, Lebedev A. Defensive Forecast for Conformal Bounded Regression. Artificial Intelligence Applications and Innovations. Volume 412, 2013, pp 384-393

3. Lebedev AV, Beyer MK, Fritze F, Westman E, Ballard C, Aarsland D. Cortical changes associated with depression and antidepressant use in Alzheimer's and dementia with Lewy bodies: an MRI surface-based morphometric study. Am J Geriatr Psychiatry, 2013. DOI: 10.1016/j.jagp.2013.02.004;

4. Lebedeva AK, Westman E, Lebedev AV, Xiaozhen L, Winblad B, Wahlund LO, Aarsland D. Structural brain changes associated with depressive symptoms in the elderly with and without Alzheimer’s disease. J Neurol Neurosurg Psychiatry, 2014. DOI: 10.1136/jnnp-2013-307110;

1. Introduction

Preliminary remarks

Oxford dictionary defines cognition as "the mental action or process of acquiring knowledge and understanding through thought, experience, and the senses" (2). Pain, tactile, visual and auditory experiences, joy, fear, beliefs, desires, attitudes, intentions – all kinds of mental phenomena pass through the "prism" of cognition. Individual differences in cognitive functions define us as individuals to a very large extent: how smart we are, how good we are at foreseeing our future, life planning, decision making, learning, emotion control, even the clarity of the text that you are currently reading is largely influenced by the author's and reader's cognitive functions.

An enigmatic boost of monkeys' cognitive abilities, so-called "cognitive revolution" that happened about 70,000 years ago, have made us humans and determined appearance and future development of science, art and other inalienable aspects of our modern life (3).

Today we live in the "golden age" for cognitive neuroscience. We have already started recovering lost cognitive abilities with a help of pharmacology, advanced brain surgery, implanting, gene therapy and engineering. Apart from this, recent advances in computer science made it possible to run simulations of certain aspects of cognition and even to share some of our cognitive abilities with computers that are rapidly becoming better and better at tasks previously thought as unfeasible for the machines, such as playing chess, natural language processing, voice and image recognition.

The main inspiration for this thesis is the hope that the fusion between neuroscience, computer science and humanism will ultimately help us to overcome a devastating burden of neurodegenerative diseases and improve quality of life in the elderly.

Cognitive impairment in the elderly and its impact on society

Multiple cognitive impairments that sufficiently affect activities of daily living manifest as dementia syndrome, which is the end-stage of many neurodegenerative diseases. Most frequently impaired domains with major impact are memory, executive, visuo-spatial functions, language and praxis.

The diseases that cause dementia tend to have a progressive course. The most frequent causes of neurodegenerative dementia – Alzheimer's and Lewy Body diseases are often co-morbid and have an age-related incidence, which, in turn, explains the rapid growth of its prevalence, associated with the population ageing (4). Thus, only in Norway, about 60000 – 70000 people suffer from dementia and this number is expected to double by 2050 (5).

It is not only patients and their caregivers who are affected by this devastating condition, but also the world society and global healthcare. Thus, financial burden of dementia is very high, equivalent to the one of heart disease and cancer (6), and set to grow exponentially over the next decades. In 2010, its total worldwide costs were estimated at 604 billion US dollars, and are expected to increase by 85 % by 2030 (7). This problem is even more serious, given that doctors specializing in age-related medicine are already in short supply, and the demand for them is becoming higher every year (8).

Several strategies to overcome these issues can be undertaken. Developing novel treatments to prevent or modify neurodegenerative diseases is probably the most crucial one. Thus, only for Alzheimer's disease, there are numerous ongoing clinical trials, the results of which will hopefully provide an opportunity to slow down or stop the disease progression. In this context, early detection and prediction of dementia is very important to select those who would have highest benefits from these trials. Importantly, one of the recent reports of Alzheimer's Disease International (ADI, the international federation of Alzheimer associations around the world) was specifically focused on the benefits of early diagnosis and interventions in AD (9). This report also suggests that early

diagnosis of AD reduces costs itself by improving institutionalization strategies and enhancing quality of life of patients and their caregivers.

All of the above, therefore, presents a need for the improved detection of cognitive impairment in the elderly at early stages, and neuroimaging is one of the most promising sources for this.

Brain Imaging

Brain imaging can be defined as a set of invasive and non-invasive techniques to image the structure, function or biochemistry of the brain. Plenty of methods are available in this field today such as magnetic resonance imaging, single-photon emission computed tomography (SPECT), positron emission tomography (PET) with different ligands including pathology-specific ones like, for example, Pittsburgh Compound B (PIB) and others (10).

Magnetic resonance imaging (MRI) is a very informative and non-invasive method. After its invention by Felix Bloch and Edward Purcell followed by Nobel Prize in 1952 it took two decades before clinical implementation of this technique became possible (11).

Today MRI is widely used for the diagnosis of dementia (10, 12), and many specialized MRI protocols and approaches to the data analysis have been developed, providing extremely wide spectrum of structural and functional information (13).

Although MRI is now implemented in the diagnostic criteria for Alzheimer's disease (14), it does not seem to reliably differentiate between all dementia types, at least with a visual assessment of anatomical MRI scans (15). Meanwhile, it is important to have a reliable differential diagnosis particularly between neurodegenerative diseases such Alzheimer's and dementia with Lewy bodies.

Brain imaging of cognitive impairment in Alzheimer's disease and dementia with Lewy bodies

A diagnostic hallmark of AD, medial temporal lobe (MTL) atrophy, has been shown to be closely associated with episodic memory impairment, which, in turn, is one of the main clinical features of the disease (16, 17) (18).

Meanwhile, emerging evidence suggests that AD may be a heterogeneous disease with several concomitant pathogeneses (19-21). Thus, neuropathological and neuroimaging studies revealed several manifestations of AD (typical, hippocampal-sparing, and limbic-predominant forms) that differ in patterns of neurofibrillary tangles distribution, brain atrophy, gender proportion, apolipoprotein E (ApoE) and microtubule-associated protein tau (MAPT) allele frequencies (20, 21), as well as several clinical manifestations that differ in the age of onset and cognitive functions affected (19, 22-24) (19, 25). A recent large-sample study performed visual assessment of atrophy patterns associated with cognitive dysfunction in multiple domains in AD. The authors found that MTL atrophy was associated with worse memory, language and attention performance, whereas "posterior atrophy" (posterior cingulate, parieto-occipital regions, precuneus) was associated with worse performance on visuospatial and executive functioning (18).

Typical brain changes associated with progression of Alzheimer's disease follow a consistent pattern affecting entorhinal cortex on early stages, then hippocampal Cornu Ammonis (CA) subfields, amygdala, and finally neocortical areas (26). This progressive atrophy can be successfully visualized *in vivo* with the help of structural MRI. Visual assessment of medial temporal lobe (MTL) atrophy on MRI scans has a substantial clinical value in detection of AD with overall accuracy higher than 80% (27-29). Its ability to predict MCI-to-AD progression, however, is varying around 60-65% (30, 31). All of the above made MTL atrophy become one of the biomarkers in proposed Dubois' criteria for prodromal AD (14).

There are also some preliminary evidences suggesting that MRI may help to differentiate AD from the second most common neurodegenerative disease in the elderly, DLB (29) (32). However, these results are limited due to different methodological frameworks and small sample sizes.

Functional MRI (fMRI) is a noninvasive technique that allows to indirectly measure brain activity, assessing changes in so-called BOLD (blood oxygenation level-dependent) signal (33). Functional MRI can be implemented within the context of cognitive tasks (e.g., comparing "baseline" and "active" conditions) or when the subject is at resting state without any particular task (34). Both task-related and resting fMRI (rs-fMRI) techniques are non-invasive, safe and have the potential to detect early brain functional abnormalities associated with cognitive impairment in the elderly, and to monitor their progression and therapeutic response. It has recently been shown that rs-fMRI may assist in differentiation between AD and DLB (35). The main limitations of BOLD fMRI, however, are substantial difficulties of signal quantification (the method usually assesses either contrast or temporal correlations of signal changes), low signal-to-noise ratio and high susceptibility to artifacts, MRI protocol differences and field strength. All of the above hampers consideration of BOLD fMRI as an imaging biomarker. On the other hand novel functional MRI techniques, such as arterial spin labeling, measuring brain perfusion are quantifiable and hold stronger potential to be used in clinical practice.

MRI can provide relevant support in the diagnosis of AD, detecting progressive atrophy, which starts from the entorhinal cortex and gradually spreads throughout the brain (12), but, as mentioned above, is currently less useful for differentiation between AD and other neurodegenerative diseases.

Although Alzheimer's and Lewy body pathologies are often present together in autopsy materials, there are strong evidences suggesting that corresponding clinical manifestations, depending on predominant pathology, demonstrate substantially different morphological profiles, primarily, with greater

involvement of hippocampal formation and related neocortical areas in AD; this may explain more severely impaired memory function in AD as compared to DLB (36-38). On the other hand, the neuropathological basis of DLB primarily includes subcortical, frontal, temporal, and parietal lobes, which in turn may explain the predominance of visuospatial, attentional, and executive function impairment in these patients (39-42). Inconsistent findings have been reported regarding the involvement of cingulate and frontal cortex in LBD compared to AD. Both post mortem (43), as well as studies using imaging techniques such as SPECT-perfusion (44), PIB-PET (45), diffusion-tensor imaging (46, 47), have reported cingulate involvement in Lewy Body dementia. There are several reports on frontal lobe atrophy in DLB (48-50). However, recent studies found orbitofrontal (51) and, on the large sample, even the whole (52) cortex to be preserved in DLB compared to AD. In addition, although there are observations from functional studies showing metabolic (53) and perfusion (54) reductions in occipital lobes in DLB compared to AD, no significant volumetric differences in this region were found (55, 56).

These findings are highly important for uncovering brain mechanisms and for understanding the pathomorphological and pathophysiological differences in these conditions.

However, whether MRI can assist in the reliable differentiation between AD and LBD is not yet clarified, mainly because most studies do not report sensitivity and specificity, providing only group differences.

Brain imaging of cognitive impairment in Parkinson's disease

Cognitive impairment is a very important and common non-motor feature of Parkinson's disease (PD) with a major impact on patients' quality of life and healthcare costs (57-59). Approximately one-fifth of newly diagnosed PD patients fulfill clinical criteria for mild cognitive impairment (PD-MCI) (60).

About one-sixth develop dementia after 5 years (61), and more than 80% of PD patients will eventually develop it as the disease progresses (62).

Although the exact role and mechanisms of the dopaminergic system in cognition are still a matter of debate, there is no doubt that its preservation is crucial for cognitive functioning of PD patients. There is strong evidence suggesting that the impairment of at least 3 major dopaminergic pathways (nigrostriatal, mesocortical, mesolimbic) originating in the brainstem play a very important role in cognitive dysfunction associated with PD (63).

Previous neuroimaging studies assessing brain networks *in vivo* have shown impairment of the dopaminergic pathways and related neural circuits in PD. Numerous studies on cognitive dysfunction associated with PD have revealed structural and functional abnormalities within the cortico-strio-thalamo-cortical circuits, known to be largely modulated by the dopaminergic system (64, 65).

Decreased 6-[^{18}F]-fluorodopa (^{18}F-DOPA) uptake in the anterior cingulate cortex, ventral striatum and right caudate nucleus has been found in PD patients with dementia (PDD) compared to PD (66). Studies employing Single Photon Emission Computed Tomography (SPECT) with the dopamine transporter-binding ligands (DaTSCAN) also suggest more severe striatal presynaptic dopaminergic deficiency in PDD compared to PD patients, especially in the caudate nuclei (67). In addition, there is also evidence suggesting an association between striatal ^{18}F-DOPA uptake and executive performance in PD patients (68-70).

Several ^{18}F-fludeoxyglucose Positron Emission Tomography (FDG-PET) studies analyzing brain networks in PD have identified partially overlapping patterns of brain metabolic changes associated with cognitive impairment in multiple domains, suggesting that the PD-related profile of cognitive impairment is associated with reduced glucose metabolism mainly in prefrontal, parietal, hippocampal and striatal regions (71-74).

$H_2{}^{15}O$-PET studies have shown an impaired basal ganglia and dorsolateral prefrontal response during executive task performance in PD (75-77).

Functional MRI studies have also revealed abnormalities within the frontal-subcortical circuits in patients with PD. For instance, an abnormal fronto-striatal response during executive task performance has been found in cognitively impaired PD patients compared to non-impaired ones (78) (79). Another fMRI study assessing working memory and motor functions in ON and OFF dopaminergic medication states in PD patients (80) found increased prefrontal and parietal activations during the working memory task performance in the OFF state, which were positively correlated with errors during the task. Studies focusing on set-shifting paradigms have found a PD-associated pattern of prefrontal and parietal response characterized by either reduced or increased activation depending on whether the caudate nucleus was involved in the task (81, 82).

Impaired deactivation of the default mode network during executive task performance has been reported in several fMRI studies of PD (83, 84). Resting state fMRI studies have reported abnormal cortico-striatal connectivity in PD (85-87), while L-DOPA administration has been shown to enhance functional connectivity in the frontal areas of the sensorimotor network (88).

Computational Neuroimaging and Computer-Aided Diagnosis

The era of computing is associated with significant changes in human life, uncovering a lot of valuable opportunities in many fields and particularly in medicine. Computational neuroimaging is a relatively new field of neuroscience and represents one of the most promising areas to provide diagnostically relevant analytic framework. Different techniques, methods and image post-processing approaches exist in this field (10, 89). Combined with pattern recognition techniques, computational approaches to structural MRI have already been shown to be effective for detection of AD, frontotemporal dementia (FTD) and mild cognitive impairment (MCI) (90-93) and hopefully will provide robust differential diagnosis in AD and DLB patients.

In this context, computer-aided diagnosis (CAD), defined as a family of computational approaches developed to assist doctors in the detection of abnormalities, quantification of disease progress and differential diagnosis (94), is a very promising subfield with high potential to be implemented in clinical practice. Potentially, it is a very cost-effective approach, since after the implementation it requires minimum technical staff to be maintained. Among other advantages of CAD is its unbiasedness toward human mistakes, global access, and possibility to establish a constantly updating large flow of the standardized data, which, in turn, may provide a very good research and clinical material for further improvements and serve as an additional incentive to implement these techniques in practice. Finally, this technology can be easily incorporated into clinical decision-support systems. However, it has its drawbacks too. One of the most critical issues pertains to the fact that use of these techniques implies a standardized process of data acquisition, which in turn requires employment of imaging protocol harmonization and preferably unified diagnostic workflows. The use of this technology by a clinician, at least at its first stages of implementation, may be associated with some technical difficulties (e.g., establishing data transfer, sending queries) and certain amount of technical training is therefore required. Lastly, its incentives and organizational governance are still a matter of research. It is worth noting though, that these issues pertain to modern healthcare in general. Thus, recent United States experience in rapid adoption of IT innovations, such as electronic health records (EHRs), in response to governmental incentive programs highlighted its problems such as a mismatch between EHR software and clinical workflow standards, which together with inadequate training and poor preparation of medical staff may lead to dissatisfaction and decreased productivity (95-97). So, the use of clinical and technical standards together with adequate personnel training is indeed a backbone of a successful adoption of any IT innovation, including CAD. Among the fields providing material for CAD in neurodegenerative diseases, brain imaging stands out as one of the most promising.

To summarize, neurodegenerative diseases have a devastating impact on society and healthcare, with increasing costs and demand for doctors who specialize in age-related medicine. Neuroimaging is an important technique that assists doctors in the diagnosis of cognitive impairment in the elderly. Some of the techniques are already being implemented in the diagnostic process. The most advanced ones (e.g., PiB PET for AD, DaTSCAN for DLB and PD) are expensive, difficult to implement and are not widely available for clinicians. It is still not clear whether MRI can help to differentiate between AD and DLB, and whether it is possible to develop a cohort-robust automated tool for solving diagnostic problems with advanced image processing and data analytical techniques.

Apart from this, brain mechanisms of cognitive deterioration associated with neurodegenerative diseases in the elderly are still a matter of debate.

Meanwhile, computational neuroimaging represents a very promising set of techniques to study mechanisms of cognitive impairment and to provide clinically relevant and automated diagnostic tools.

2. Objectives

1) To investigate brain changes underlying cognitive impairment in neurodegenerative diseases (Alzheimer's, Lewy body dementia and Parkinson's disease).
2) To assess the applicability of pattern recognition techniques for:
   a) Differential diagnosis of cognitive impairment
   b) Prediction of further cognitive deterioration in patients with mild cognitive impairment;
3) To investigate problems associated with implementation of computer-aided image-based tools for detection, prediction and differential diagnosis of cognitive impairment.

3. Hypotheses

1. With the help of computational neuroimaging, accurate and cohort-robust tools can be developed to assist in the differential diagnosis and early detection of cognitive impairment in the elderly;

2. Cognitive impairment in Parkinson's disease is associated with structural and functional abnormalities within temporo-parietal and prefrontal circuits;

3. Brain dynamics underlying cognitive functioning in PD is influenced by nigrostriatal dopamine deficiency.

4. Methods

4.1 Cohorts

In the present project 5 cohorts were used. Their description is summarized in the **Table M-1** and in the subsequent paragraphs.

Table M-1. Characteristics of the cohorts

	DemWest	Slo	ADNI	AddNeuroMed	PPMI
Papers	I		II		III, IV
Total N	63	34	808	321	179
Diagnoses	AD, DLB	AD, DLB, PDD	AD, MCI, HC		PD-MCI, PD-NC, HC
Imaging Modalities	MRI, DaTSCAN	MRI, DaTSCAN	MRI (with harmonized protocol)		MRI, fMRI, DaTSCAN
Cognitive tests	MMSE, CDR, CVLT-II, VF, BNT, BLOT, BFRT, ROCFT, ST		MMSE, CDR, ADAS, ANART, RAVLT, SF, WAIS-R, BNT, TMT, SDMT		MoCA, HVLT-R, SF, BLOT, LNST, SDMT
Country	Norway	Slovenia	North America	Europe (Finland, Poland,Italy, Greece, UK, France)	USA, Europe and Australia

AD - Alzheimer's Disease, DLB - Dementia with Lewy bodies, PDD - Parkinson's Disease Dementia, MCI - Mild Cognitive Impairment, PD - Parkinson's Disease, NC - Normal Cognition, HC - Healthy Controls;

ADAS - Alzheimer's Disease Assessment Scale (cognitive subscale), ANART - American National Adult Reading Test, BFRT - Benton Facial Recognition Test, BLOT - Benton Line Orientation Test, BNT - Boston Naming Test, CDR - Clinical Dementia Rating scale, CVLT-II - California Verbal Learning Test (II), DS - Digit Span test, HVLT-R - Hopkins Verbal Learning Test (Revised), MMSE - Mini Mental State Examination, MoCA - Montreal Cognitive Assessment, RAVLT - Rey Auditory Verbal Learning Test, ROCFT- Rey-Osterrieth Complex Figure Test, SDMT - Symbol Digit Modalities Test, SF - Semantic Fluency, ST - Stroop Test, TMT - Trail Making Test, VF - Verbal Fluency, WAIS-R - Wechsler Adult Intelligence Scale (Revised).

1) DemWest (Paper 1)

This cohort is based on a population drawn from the Dementia Study in Western Norway - DemWest. In this study, all patients referred to the geriatric psychiatry and geriatric medicine clinics in Western Norway during 2005-2007 were considered for inclusion. Neurology clinics were asked to refer potential candidates to the study. Patients with a new diagnosis of mild dementia, without confusion or previous history psychotic disorders were invited. Patients were diagnosed as probable AD according to NINCDS-ADRDA (National Institute of Neurological and Communicative Diseases and Stroke-Alzheimer's Disease and Related Disorders Association), Parkinson's disease dementia (98), or DLB (1). The exclusion criteria were normal cognition or mild cognitive impairment, moderate or severe dementia defined as MMSE < 20, recent major physical disease, previous affective or psychotic disorder. After 2007, only DLB and PDD patients were included, with MMSE between 16-20.

Routine physical examination and blood tests were performed for all patients, a subgroup underwent lumbar puncture for CSF analyses, and ECG was performed if clinically indicated.

A comprehensive battery of standardized clinical assessment instruments was administered at baseline and annually, assessing cognitive, psychiatric, and motor functions, including a battery of neuropsychological tests. Details of the selection and diagnostic procedures have been reported previously (99).

The Montgomery-Asberg Depression Rating Scale (MADRS) was administered by trained study physicians (geriatric psychiatrists or geriatricians) to evaluate depression.

For most patients with suspected DLB single photon emission computed tomography (SPECT) procedures with ^{123}I-FP-CIT compound (DaTSCAN) were performed. SPECT images were acquired at three institutions on Siemens Symbia and E-Cam dual-head Gamma cameras with similar protocols. Transversal images through the basal ganglia were visually analyzed by one nuclear medicine specialist blinded to all patient information.

MRI Images were collected from three centres with harmonized protocols using T1-weighted 3D series. The subjects were scanned on 1.5 Tesla MRI scanners at 3 different sites: Stavanger, Haugesund (Philips Intera) and Bergen (GE Signa Excite).

Reliability assessment

In order to check intra- and inter-scanner reliability in the DemWest cohort, we performed a validation study using human phantom scanning. For this purpose, MRI was performed in three healthy subjects with repeat scanning including FLAIR and 3D T1 two times at each center on the same day. The MRI procedures included two scanning sessions with a pause in between when the subject left the MRI room. Human phantom scanning was completed within 3 months for all participating centers.

The analysis included estimation of intra- and inter- scanner reliability coefficients (Cronbach's alpha) for intracranial volume (ICV) and mean cortical thickness (MCT) measurements.

Reliability assessment was performed using the ''ltm'' (Latent Trait Models) package (100) in R programming language (101), which is well established and freely available for download (http://www.R-project.org/).

Estimation of the reliability coefficient (Cronbach's alpha) showed appropriate results: the intra-/inter-scanner reliability coefficients for ICV and MT were 0.996/0.995 (excellent) and 0.945/0.752 (excellent/acceptable) respectively. This allowed us to use the images from all three participating centers.

The study was approved by Regional Committee for Medical Research Ethics in Western Norway, and received financial support from the Western Norway regional health authority and the Norwegian Research Council. All patients signed informed consent to participate in the study.

2) Slovenian AD and DLB cohort (paper I)

The cohort consisted of dementia patients attending the memory outpatient clinic at the Department of neurology (University Medical Centre in Ljubljana). The diagnosis of dementia was made according to DSM-IV criteria and the diagnosis for AD was based on The National Institute of Neurological and Communicative Disorders and Stroke-Alzheimer's Disease and Related Disorders Association (102). DLB was diagnosed according to the revised consensus criteria (1) in the DemWest cohort and the 1996-criteria for the Slovenian (Slo) cohort (37). For the Slo cohort we merged DLB and PDD patients (103), since these syndromes share clinical and pathological features (104).

Standardized clinical screening assessment instruments were administered in both cohorts to assess cognitive, psychiatric, and motor functions. Clinical assessment was performed using Mini Mental State Examination (MMSE), Unified Parkinson Disease Rating Scale, Clinical Dementia Rating scale, Neuropsychiatric Inventory and Beck Depression Inventory, detailed neuropsychological test battery (Delis-Kaplan Executive Function System, California Verbal Learning Test II, verbal fluency test, Boston Naming Test, The Rey-Osterrieth Complex Figure Test, Benton Line Orientation Test, Benton face recognition test, Stroop test), tests of autonomic functions and assessment of daily activities. In addition to routine blood tests, laboratory assessment of thyroid function, vitamin B12 and folate (the patients with vitamin deficiency were excluded) was administered. In both cohorts, visual assessment of MRI scans (both T1 and T2-FLAIR) were performed to exclude structural pathologies other than AD or DLB that could account for the symptoms. Routine physical examination was also performed.

DaTSCAN images were acquired for all patients on Siemens Symbia T2 dual-head Gamma camera and were evaluated by two independent raters (the first one is a specialist in nuclear medicine and the second one is a neurologist with additional knowledge in functional brain imaging). They were blinded for the

clinical information. Normal/abnormal tracer uptake patterns were analyzed. The results were similar in the DLB and PDD patients.

The study was approved by the local Regional Committee for Medical Research Ethics. All patients provided written consent to participate in the study after the study procedures had been explained in detail to the patient and a caregiver.

3) ADNI (paper II)

Alzheimer's Disease Neuroimaging Initiative (ADNI) launched in 2004 and was aimed at discovering more sensitive and accurate biomarkers for Alzheimer's disease and its progression at earlier stages.

To date, ADNI is the largest project of its kind, covering thousands of patients at different stages of AD and healthy controls. More than 50 centers participate in this initiative, to date.

In total, 808 subjects aged between 55-90 years were enrolled in the ADNI-1 cohort used in our project.

Normal subjects had to have MMSE scores above 24, a CDR of 0, had not to have clinical depression, MCI or severe cognitive impairment.

MCI subjects had to have MMSE scores between 24-30, memory complaints and objective memory loss (measured by education adjusted scores on Wechsler Memory Scale Logical Memory II), a CDR score of 0.5, absence of significant levels of impairment in other cognitive domains, preserved activities of daily living, and an absence of dementia.

Patients with mild AD had MMSE scores between 20-26, CDR of 0.5 or 1.0, and met NINCDS/ADRDA criteria for probable AD.

Neuropsychological battery included Alzheimer's Disease Assessment Scale (cognitive subscale) (ADAS-Cog), American National Adult Reading Test (ANART), BNT - Boston Naming Test, Digit Span test (DS), Rey Auditory

Verbal Learning Test (RAVLT), Semantic Fluency (SF), Trail Making Test (TMT), Wechsler Adult Intelligence Scale (Revised) (WAIS-R). For more details, please visit http://www.adni-info.org/Scientists/ADNIStudyProcedures.aspx.

All subjects had clinical assessments, physical examination and 1.5 T structural MRI (acquired with harmonized protocols) at specified intervals for 1-5 years.

The ADNI project is conducted according to Good Clinical Practice guidelines, the Declaration of Helsinki, US 21CFR Part 50 – Protection of Human Subjects, and Part 56 – Institutional Review Boards. Written informed consent for the study was obtained from all subjects and/or authorized representatives and study partners.

4) AddNeuroMed (paper II)

The study included six centers at University of Kuopio, Finland; University of Perugia, Italy; Aristotle University of Thessaloniki, Greece; King's College London, United Kingdom; University of Lodz, Poland; and University of Toulouse, France. The Karolinska Institutet (Stockholm, Sweden) was established as the center for image repository, quality control, and overall coordination site.

Two hundred and twenty one subjects with AD (n=107), 114 MCI (n=114) and 100 HCs were included. Informed consent was obtained for all subjects, protocols and procedures were approved by the local data acquisition site and the data coordination center.

Imaging and clinical protocols were harmonized with the ADNI study (see above). For more details see http://www.innomed-addneuromed.com and (105).

Exclusion criteria included other neurological or psychiatric disease, significant unstable systemic illness or organ failure, and alcohol or substance misuse.

The project was approved by local Ethical Committees at all participating centers. Written consent to participate was obtained from all patients and/or caregivers.

5) PPMI (papers III-IV)

Parkinson's Progression Markers Initiative (PPMI) is a large-scale international project aimed at discovering novel biomarkers for Parkinson's disease and its progression. The study launched at 21 clinical sites in the United States, Europe, and Australia. For details, please see (106).

To date, more than 450 patients at different stages of PD and more than 250 healthy controls are included from more than 30 centers throughout the world.

Inclusion criteria required that subjects must have at least two of the following symptoms: resting tremor, bradykinesia, rigidity or either asymmetric resting tremor or asymmetric bradykinesia. In addition, the subjects had to have Hoehn and Yahr stage I or II at baseline, and a pathological ^{123}I-FP-CIT SPECT scan.

Exclusion criteria were atypical PD syndromes due to drugs or metabolic disorders, encephalitis, or other degenerative diseases. In addition, it was required that the subject was not taking levodopa, DA agonists, MAO-B inhibitors, amantadine or other Parkinson's disease medication; or had taken levodopa or dopamine agonists prior to baseline for more than a total of 60 days.

This cohort was used in 2 studies assessing brain structural and functional correlates of cognitive impairment in PD. Therefore, a more detailed description of cognitive battery is provided below.

Neuropsychological assessment

In addition to a cognitive screening test, the Montreal Cognitive Assessment (MoCA), all subjects underwent a neuropsychological test battery developed to assess major cognitive domains affected by PD.

Visuospatial function was evaluated using the 15-item version of the Benton's Judgment of Line Orientation Test, which examines the ability of a subject to estimate angular relationships between line segments by visually matching angled line pairs to 11 numbered radii forming a semi-circle (107).

Verbal memory was assessed using the Hopkins Verbal Learning Test-Revised (HVLT-R) (108), which consists of presenting a list of 12 words over three learning trials. With each repetition, subjects are expected to learn additional words on the list and increase their performance with each trial. Total immediate recall or encoding (sum of trial 1-3) and delayed recall (after 20-25 minutes) scores were included in this study.

Executive functions were evaluated using three semantic fluency tests (names of animals, fruits and vegetables, in one minute each), the MoCA subtests of phonemic fluency (words that start from the letter "F", in one minute) and alternating trail making (drawing a line, going from a number to a letter, in ascending order; score 0-1).

Attention was assessed by the Letter-Number Sequencing Test (LNST), in which a combination of numbers and letters is read to the subject who is then asked to recall the numbers, first in ascending order and then the letters in alphabetical order. The Symbol Digit Modalities Test (SDMT) was also used to assess attention, in which specific numbers had to be paired with geometric figures based on a reference key within 90 seconds.

Diagnosis of MCI

For the study III, we performed the classification of MCI by an approximation to the guidelines of the Movement Disorders Society (MDS) Task Force for the level II diagnosis of PD-MCI (109). Since the PPMI study was launched before these guidelines had been published, some adjustments had to be made. Therefore, the MoCA items were included for the assessment of the five cognitive domains: attention and working memory, executive, language, memory

and visuospatial. PD patients were classified as PD-MCI if they showed impairment in two or more tests or items within the same cognitive domain or in two or more domains. Impairment was defined as a score below 2.0 standard deviations (SD) for the individual continuous tests or a score below the maximum for the ordinal and categorical items. Based on previous recommendations made by the MDS Task Force criteria for PDD (110), patients were considered to be impaired if they scored below the maximum score on the items of MoCA.

Cognitive Domains

Three cognitive domains were calculated based on the standardized tests for memory, visuospatial and attention/executive functioning. Raw values were converted to z-scores using the mean and standard deviation of the healthy control group. Domain composite scores were calculated by averaging z-scores of the standardized tests in each cognitive domain.

In the memory domain, three learning trials and the delayed recall of HVLT-R were included. The visuospatial domain included the Benton judgment of line orientation. The attention/executive domain included the LNST, SDMT, semantic fluency and the phonemic fluency test. No corrections were performed to adjust the tests scores for age or gender given that the subsequent analyses included these variables as nuisances.

Since the calculated composite scores for cognitive domains were scaled and reflected positive cognitive performance (the higher the score, the better functioning in a corresponding domain), we defined the “motor” domain by inverting and scaling UPDRS-III raw scores in order to achieve the same variable scale and direction (higher scores correspond to better motor function) when assessing and plotting the results.

MRI

A standardized MRI protocol included acquisition of whole-brain structural and functional scans on 3 Tesla Siemens Trio Tim MR system.

3D T1 structural images were acquired in a sagittal orientation using a MPRAGE GRAPPA protocol with Repetition Time (TR) = 2300 ms, Echo Time (TE) = 2.98 ms, Field of View (FoV) = 256 mm, Flip Angle (FA) = 9° and 1 mm^3 isotropic voxel.

For each subject, 212 BOLD echo-planar rs-fMRI images (40 slices each, ascending direction) were acquired during a 8 min, 29 sec scanning session (acquisition parameters: TR = 2400 ms, TE = 25 ms, FoV = 222 mm, FA = 80° and 3.3 mm^3 isotropic voxels). Subjects were instructed to rest quietly, keeping their eyes open and not to fall asleep.

More details can be found in the MRI technical operations manual at http://www.ppmi-info.org/.

DaTSCAN

^{123}I-FP-CIT SPECT was performed at the screening visit. Images were acquired 4 ± 0.5 hours after injection of [123I]FP-CIT (111) with a target dose of 185 MBq. The radiopharmaceutical was provided as a unit dose and filled to a standard volume, which was re-assayed.

Specific acquisition parameters such as collimation were selected for each center at a preceding technical visit.

Raw projection data were acquired into a 128 x 128 matrix with steps of 3 or 4 degrees for the total projections. Image preprocessing (reconstruction, attenuation correction, spatial normalization) was performed using the Hermes software (Medical Solutions, Stockholm, Sweden) at a central SPECT Core lab in New Haven (Connecticut, United States). Specific binding ratios were

calculated for the left and right caudate nuclei according to specific binding ratio = (L/R Caudate)/(Occipital area)-1 and then averaged for further analysis.

The study presented no risks or harm to participants, confidentiality and anonymity were maintained within the legal context of the country, written consent was obtained from all subject after the detailed explanation of study procedures, approved by Institutional Review Board (Independent Ethics Committee).

4.2 Image Preprocessing

Surface-based framework (Papers I-III)

Reconstruction of the brain cortex was performed using the Freesurfer software (v 5.1) installed on CentOS 5.6 x86-64 workstation. The software is freely available for download online (http://surfer.nmr.mgh.harvard.edu). The image preprocessing details are described in prior publications (112-116). In short, the pipeline includes skull stripping and removal of non-brain soft tissues with a hybrid watershed/surface deformation procedure (117), automated Talairach transformation, intensity normalization (118), tessellation of the gray matter white matter boundary, topology correction (119), and surface deformation to optimally place the gray/white and gray/cerebrospinal fluid borders (112, 114). After the cortical reconstruction, a number of deformable procedures are performed: surface inflation (120), registration to a spherical atlas utilizing individual cortical folding patterns to match cortical geometry across subjects (116), parcellation of the cerebral cortex into units based on gyral and sulcal characteristics (113, 121). This method uses both intensity and continuity information from the whole three-dimensional MR volume during segmentation and deformation procedures to produce representations of cortical thickness, calculated as the closest distance from the gray/white boundary to the gray/CSF boundary at each vertex on the tessellated surface (114). The maps are generated

using spatial intensity gradients across tissue classes and are not reliant only on absolute signal intensity. The maps produced are able to detect submillimeter differences between groups. Procedures for the measurement of cortical thickness have been validated against histological analysis (122) and manual measurements (123, 124). Freesurfer morphometric procedures have been demonstrated to show good test-retest reliability across scanner manufacturers and across field strengths (125).

The described surface-based pipeline produced several morphometric modalities: cortical thickness (papers I, II, III), Jacobian maps (paper II), sulcal depth (paper II).

At the final step, 327684 normalized measurements acquired for every subject were concatenated into large matrices (one for each high-dimensional morphometric modality).

41 volumetric measurements for all subjects (paper II) were corrected for intracranial volume (ICV) using linear modeling (removing linear effects of ICV) and finally concatenated into a n-by-41 matrix that was used in the subsequent analysis.

Of note, the Freesurfer output for all subjects underwent visual quality control and misclassified areas (mainly, regions near cerebellar sinuses and orbitofrontal cortex) were corrected manually, blindly to the clinical diagnosis.

Semi-automated quantification of striatal dopamine transporter binding ratio (paper IV)

The DaTSCAN images were reconstructed using iterative reconstruction algorithm as implemented in the Hermes software (Medical Solutions, Stockholm, Sweden) at a central SPECT Core lab in New Haven (Connecticut, United States). Chang 0 attenuation correction was applied using an empirically derived attenuation coefficient, μ, based on measurement at the scanners during the preceding technical site visit. Finally, the image volumes were spatially

normalized using the mentioned software and a standardized volume of interest template was used to determine the spatial location of the right and left caudate nucleus and putamen, as well as occipital reference regions. Specific binding ratios were calculated for the left and right caudate nucleus and putamen according to specific binding ratio=(striatal region)/(occipital)-1.

Voxel-based framework (paper IV)

As a first step, a population template was generated from the bias-corrected T1 structural images using the Diffeomorphic Anatomical Registration Through Exponentiated Lie Algebra (DARTEL) algorithm (126) in order to improve normalization quality.

For the fMRI data, two initial echo-planar volumes were automatically removed by the scanner software to minimize T1 effects on the T2* echo-planar images, and the remaining 210 volumes underwent preprocessing in the SPM8-based (http://www.fil.ion.ucl.ac.uk/spm) pipeline implemented in the Data Processing Assistant for Resting-State fMRI: Advanced Edition (DPARSFA, version 2.3) (127), installed within the MATLAB environment (128).

Next, functional images underwent the following preprocessing steps: spatial realignment and slice-timing correction, co-registration with the high-resolution structural scans. Finally, the co-registered BOLD volumes were normalized into standardized Montreal Neurological Institute (MNI) space using the DARTEL template and resampled to 3 mm^3 isotropic voxels. Spurious variance was reduced by a voxel-specific head motion correction (129) and by regressing-out time-series from the white matter and cerebrospinal fluid. Next, the images were smoothed with a 2 mm^3 Gaussian kernel, band-pass filtered to eliminate biologically non-relevant signals (130, 131) and the resulting low-frequency fluctuations were extracted from 90 regions-of-interest defined in the Automated Anatomical Labeling (AAL) atlas (132) and were used in the subsequent network analysis (133).

4.3 Statistical Analysis

Paper I

A multivariate analysis of surface-based cortical thickness measurements was performed using "spls" (Sparse Partial Least Squares) R-package (version 2.1); its methodology has been described elsewhere (134, 135), and the documentation is available via the following link: http://cran.r-project.org/web/packages/spls/spls.pdf. The general principle of this methodology is to impose Least Angle Regression (LARS) algorithm for the variable selection within the context of partial least squares (135).

Applying LARS algorithm for the variable selection by penalizing loadings we end up with two adjusting parameters: 'eta' – the measure of sparsity (varying between 0 and 1; when 'eta' is 0, regular PLS is used) and 'K' – the number of latent variables. For the details see (135).

We chose these parameters within a preliminary specified range (1–5 for 'K' and 0–0.5 with the increment of 0.1 for 'eta'). We limited our search by 5 latent variables (K), since after this point we did not observe significant increase of the explained variance percentage, and 'eta' value limit was set to 0.5, because, according to our previous observations, higher values produce oversmoothed models. We applied the described approach for several smoothing kernels of 0, 5, 10, 15, 20 and 25 FWHM (Full Width at Half Maximum) after removing age-related effects.

For each FWHM the best model had been selected based on its mean squared error of prediction (MSPE), whereupon the models' Leave-one–out (LOO) cross-validated sensitivity and specificity as well as their performance on the independent dataset of 27 AD subjects were compared.

After choosing the best model we plotted its sensitivity and specificity and calculated area under the ROC curve (AUC). When reporting sensitivity and specificity, we used 0.5 as a cut-off value, which was the middle point between

the minimum (0) and maximum (1) likelihoods for Lewy Body Pathology across the all models.

Finally, we mapped the variable coefficients from the best model into the brain space in order to define the regions, which were the most relevant for the AD/DLB classification.

Paper II

Statistical analysis was carried out using the R programming language (R Core Team, 2012)(101), version 2.15.1, on R-Cloud built on EBI 64-bit Linux Cluster (136). Demographic and clinical features were compared using parametric and non-parametric tests as appropriate. Principal component analysis (PCA) from the R 'base' package was used with visual inspection of PCA score-plot for the outlier detection (137). One subject was excluded during this procedure. The 'randomForest' package (138) was used in further analysis.

The Random Forest algorithm is formally defined as a collection of tree-structured classifiers: $f(x, \theta_k), k = 1, 2, \dots, K$; where θ_k are random vectors that meet i.i.d. (independent and identically distributed) assumption (139) and each tree casts a unit vote for the most popular class at input x (140). For classification problems, the forest prediction is the unweighted plurality of class votes (majority vote). The algorithm converges with a large enough number of trees. For more detailed explanation see (140).

The R package 'caret' (141) was used to implement recursive feature elimination (RFE) based on Gini-criterion with 5-fold cross-validation (CV) within the context of RF (142). Each of the steps described below were performed for all modalities: cortical thickness, sulcal depth, Jacobian maps, non-cortical volumes, combined parcellated measurements of cortical thickness and non-cortical volumes. First, the measurements with near-zero variance were removed from the feature sets and the resulting output underwent stepwise RFE. 10 000 trees were used to "grow" the first forest (using full feature set), and afterwards RFE

was performed based on feature importance vector (defined in Eq. 2) derived from the first forest, by removing lowest-ranked 5% of the features at each step (gradually reducing the dimensionality as 100%, 95%, … etc., up to 50%), and by the subsequent accuracy comparison with 5-fold CV. In order to reduce CPU, RAM and time usage the forests were trained with 1000 trees (instead of 10 000 for the first forest) at each step of RFE. After selection of the optimal feature subset, m_{try}-parameter adjustment was also performed using 1000 trees (search range $\in [\frac{\sqrt{N_{features}}}{4} ; \sqrt{N_{features}} * 2.5]$, step = $\frac{\sqrt{N_{features}}}{4}$), and finally the forests were retrained with optimal parameters using 10 000 trees. For the parcellated data (non-cortical volumes and parcellated thickness), an exhaustive search for optimal feature subset and m_{try}-parameter was performed, "growing" 1000 trees at each step with 10-fold CV.

The following parameters from the final models were reported to characterize performance: out-of-bag error [for the term definition see (140)], area under the ROC curve (AUC), sensitivity/specificity and overall accuracy on the testing datasets of AD, HC and MCI subjects (see "Subsampling"). ROC-curves of the best models were compared using DeLong's test for two correlated ROCs, as implemented in the 'pROC' R-package (143).

The robustness of each model was also tested with respect to cohort differences (using a different cohort of AD and HC subjects from the AddNeuroMed study (105).

Finally, *variables of importance* were mapped from the best model into the brain space in order to identify the regions, which were most relevant for the classification.

The classifiers trained with individual morphometric modality were combined by a majority vote and subsequently compared with the best model that demonstrated the highest accuracy (the one trained using parcellated thickness and volumetric measurements) on the test set.

To investigate the effect of different atlases, we selected cortical thickness as a measurement type that produced the most accurate models and applied two parcellations implemented in the Freesurfer package – *Desikan-Killiany (DK)* and *Destrieux (D)* atlases – to extract averaged values from the predefined regions.

Paper III

Analyses of clinical and behavioral data were carried out using SPSS 20.0. Differences between groups in demographic, socio-demographic, clinical and neuropsychological variables were analyzed using Mann-Whitney U tests for non-normally distributed data (as indicated by the Kolmogorov-Smirnov test), student's T-test for normally distributed data, and Chi-squared X^2 for categorical data. Proportions with 95% CI were also calculated.

The analyses involving neuroimaging data were performed in FreeSurfer. In particular, differences in cortical thickness between controls, PD with normal cognition (PD-CN) and PD-MCI were examined on the cortical surface maps vertex by vertex using a general linear model. Confounding variables such as age, gender, education, MRI software version (syngo MR B15 or syngo MR B17) and scanner (Siemens Tim Trio or Siemens Verio) were included as covariates in these analyses to ensure they did not contribute to any group differences. In addition, for the PD-CN and PD-MCI group comparisons, the UPDRS III total scores were also included as additional covariates. To assess the neuroanatomical substrates of cognitive impairment, correlation analyses between cortical surface maps and cognition were also carried out, while adjusting for the previous covariates. First, we performed correlations between cortical thickness and the z-scores of the three cognitive domains. In addition, since by combining tests into domain some specific information might be lost, we also correlated cortical thickness with z-scores of the individual continuous cognitive tests. In all imaging analyses, cluster-wise correction using Monte

Carlo simulation with 10.000 iterations (vertex-wise threshold of $p < 0.05$) was applied in order to control for multiple comparisons.

Paper IV

Automated meta-analysis

In order to support our hypotheses and to objectively identify regions that are relevant for cognitive functions, an automated search using the meta-analytical software Neurosynth (http://neurosynth.org) was undertaken (see **Figure M-1**). This approach utilizes text-mining and machine-learning techniques to perform probabilistic mapping between neural and cognitive states (144). In the present study, the Python-based version (https://github.com/neurosynth/neurosynth) was used. The database was accessed on 24.10.13, searching for the key-words "executive" (237 studies), "visuospatial" (n=116) and "memory" (n=1470).

After the search overlapping patterns were found between cognitive domains. They were in line with the regions that have revealed an association with cognitive impairment in PD highlighted in the introduction. Thus, the profile of visuospatial functions included prefrontal, parietal and occipital regions. The "executive" pattern contained prefrontal (with more extended involvement of DLPFC), cingulate, superior parietal, temporo-occipital, basal ganglia and cerebellar regions. Finally, the "memory" profile, in addition to prefrontal and parietal regions, also included hippocampus, temporal areas and basal ganglia.

Due to the observed overlap, the resulting statistical maps were merged and overlaid with the Automated Anatomical Labeling (AAL) atlas in order to have an unbiased definition of ROIs associated with cognitive functions for further network analysis.

Network Analysis

The data analysis workflow was developed in order to assess both regional and global network-level correlates of presynaptic DAT uptake and cognitive

functions. To do this, two metrics were selected: *nodal strength* (local measure) and *modularity* of a network (global measure).

The Brain Connectivity Toolbox (BCT, http://www.brain-connectivity-toolbox.net) (133) was used to compute the described measures. Of note, connectivity matrices were neither thresholded nor binarized. Instead we employed a strategy that aimed to analyze weighted graphs by taking into account both positive and negative weights.

Next, the analysis proceeded in two directions with the aim of assessing local and global network-level correlates of cognitive functioning in PD and the impact of nigrostriatal dopaminergic deficiency on these networks.

All statistical analyses were performed using the R programming language (R Core Team, 2012)(101).

Partial Least Squares Regression (PLSR) was performed to reduce the dimensionality of the data, estimating latent components associated with composite scores for each domain (executive, memory, visuospatial).

PLSR is an effective data-driven method that allows high-dimensional associations between explanatory and response variables to be reduced into a small set of latent variables (LVs) (145). After decomposition, each of the LVs represents a distinct pattern of brain–behavior associations.

The following elements of these components were of particular interest in our study: (1) eigenvector (loadings) showing the degree to which a given latent variable contributes to the variance within the X-matrix (in our case, brain network measures), and (2) a set of scores representing a transform of a particular data-point into a latent component's space (the degree to which a given component is "represented" in a particular subject).

The models were assessed with leave-one-out cross-validation. As a result, 3 LVs minimizing total Root Mean Squared Error Prediction (RMSEP) for all 3 domains were selected. Individual LV scores were subsequently correlated with 3 cognitive domains using motor function, age and sex as nuisance covariates.

GLM formula:

LV_N-score ~ (executive domain) + (memory domain) + (visuospatial domain) + (motor domain) + (age) + (sex).

Finally, the scores were correlated with mean caudate DaT binding ratios in order to investigate which of them were influenced by nigrostriatal dopamine deficiency. The analysis was focused only on the caudate nuclei (without putamen), as this striatal structure is well documented to be involved in cognition.

Impact of nigrostriatal deficiency on the modularity of cognitive brain circuitry.

For the second part, adjacency matrices were constructed using 60 AAL ROIs identified during the meta-analysis step. Next, modularity was estimated based on both negative and positive weights (as described in Eq. 2a and 2b).

Finally, an association between network modularity and mean DaT uptake in the caudate nuclei was analyzed using linear modeling.

5. Results

Within this project, we studied 1240 patients with Alzheimer's, Parkinson's disease, Lewy body dementia and mild cognitive impairment, and 325 healthy controls, in total (See **Table M-1**).

5.1 Paper I

SPLS Classification: AD vs DLB

During the search for the optimal model we observed optimal performance for FWHM of 20 mm in both cohorts. 'K'/'eta' parameters were set as 2/0.3 for the first (Dem- West) cohort and 2/0.4 for the second (Slo) cohort, respectively. Sensitivity/specificity/AUC for AD/DLB were 94.4/ 88.89 %/0.978 for the DemWest cohort and 88.2/94.1 %/0.969 for the Slo cohort (see **Figure 1.1**). Overall accuracies were 91.64 and 91.15 in the training DemWest and Slo datasets, respectively. Additionally, 21 out of 27 probable AD subjects from the independent dataset of the DemWest cohort were correctly classified by the corresponding model (accuracy = 77.78 %), suggesting appropriate generalization.

In the mixed cohort, 'K'/'eta' parameters were set as 2/0.4. sensitivity/specificity/AUC were 82.1/85.7 %/0.948 for the training and 77.8/75 %/0.731 for testing datasets (overall accuracies were 83.9 and 76.4, respectively).

As expected, when tested on data from different cohorts (DemWest models on Slo data and vice versa) the models failed to produce appropriate accuracy. Thus, the DemWest model showed 0.59/0.59/ 0.67 for sensitivity/specificity/AUC on the Slo data, and the Slo model demonstrated 0.61/56/0.56 on the DemWest data, respectively.

Figure 1.1. SPLS model performance.

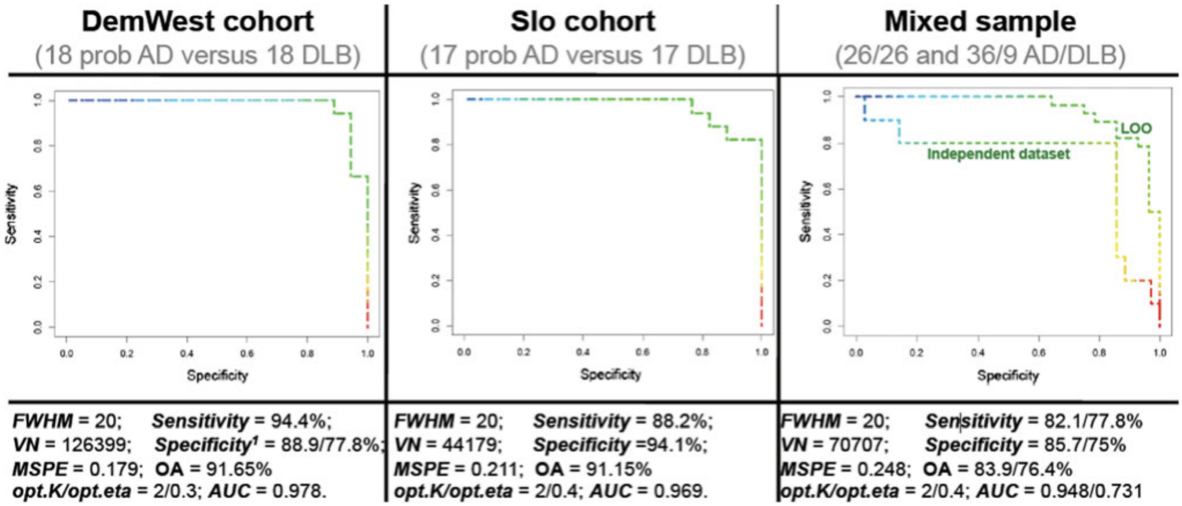

The graphs are the ROC curves for the classifiers in two cohorts (DemWest, Slo) and in the mixed sample, consisted of the equivalently combined training dataset (26/ 26 AD and DLB patients) and of the independent dataset (remaining 36/9 AD/DLB cases). Leave-one-out cross validation performance is plotted for each model. For the mixed sample, classifier performance on the independent dataset is also provided. FWHM full width at half maximum (smoothing kernel), VN number of the selected features (vertices), opt.K/opt.eta optimal 'K' (number of latent components) and 'eta' (sparsity) parameters, MSPE mean squared prediction error, AUC area under the ROC curve.

Regions of relevance for AD/DLB classification

Mapping the coefficients into the brain space revealed several regions, which appeared to be the most relevant for the classification. The pattern of difference was similar in all cohorts (**Figure 1.2**). Cortical thinning, which increased the chances for the subject to be classified as an AD patient, was observed bilaterally in anterior parahippocampal region and temporal pole (the most relevant areas), subcallosal (subgenual cingulate) and occipital regions.

Figure 1.2. Regions of relevance for AD/DLB classification.

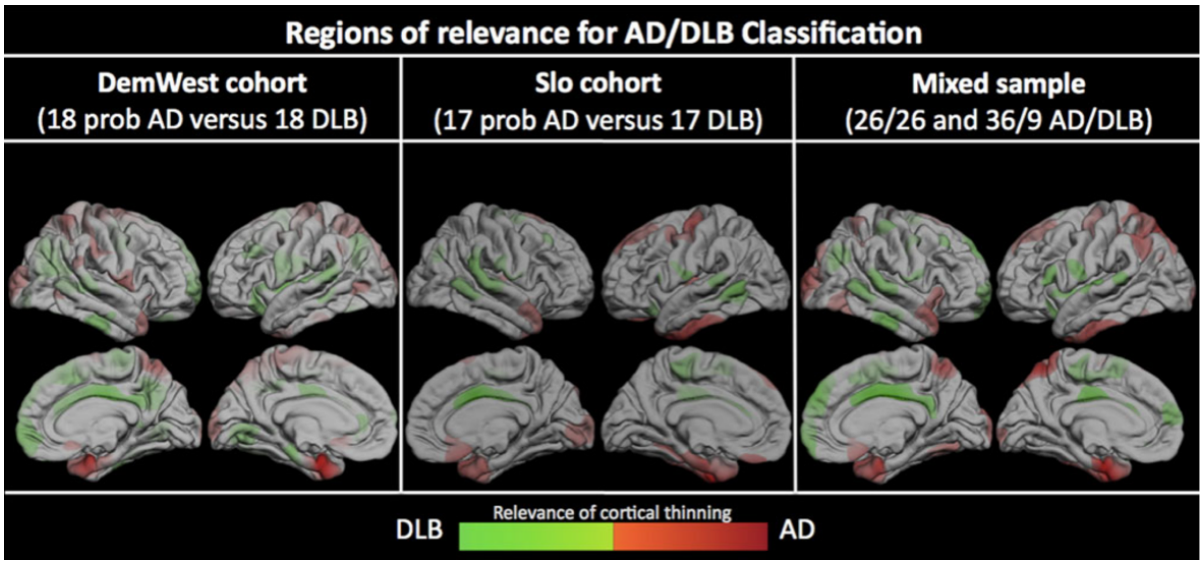

The figure shows regions of relevance for AD/DLB classification from three models obtained in DemWest, Slo and mixed cohorts. The last sample consisted of the equivalently combined training dataset (26 AD and 26 DLB patients) and of the independent dataset (remaining 36/9 AD/ DLB cases). Red spectrum reflects pattern of cortical thinning that increased chances for the subject to be classified as an AD patient. Green spectrum is the regions of importance for DLB.

Cortical thinning relevant for DLB was observed bilaterally in the cingulate region (affecting middle and posterior parts on the right side and middle on the left), superior temporo-occipital areas, and lateral orbitofrontal cortex.

In the DemWest and in the mixed sample, AD-associated patterns also included changes in the parietal region, whereas DLB-supportive thinning was additionally found in insular area. This was not observed in the Slo cohort.

5.2 Paper II

AD/HC Classification

Three models had competing performances on the testing set (**Figure 2.1**). The model trained using high-dimensional thickness measurements demonstrated AD-detection sensitivity/specificity of 88.6%/90.7%, its AUC (95% C.I.) was 0.93 (0.9-0.96); while the model trained using *volumetric measurements* resulted in sensitivity/specificity = 82.9%/86.7%, AUC = 0.91 (0.88-0.95); and using parcellated measurements of cortical thickness and subcortical structures resulted in sensitivity/specificity = 88.6%/92.0%, AUC = 0.94 (0.91-0.96).

Figure 2.1. ROC curves: Morphometric Modalities (AD/HC)

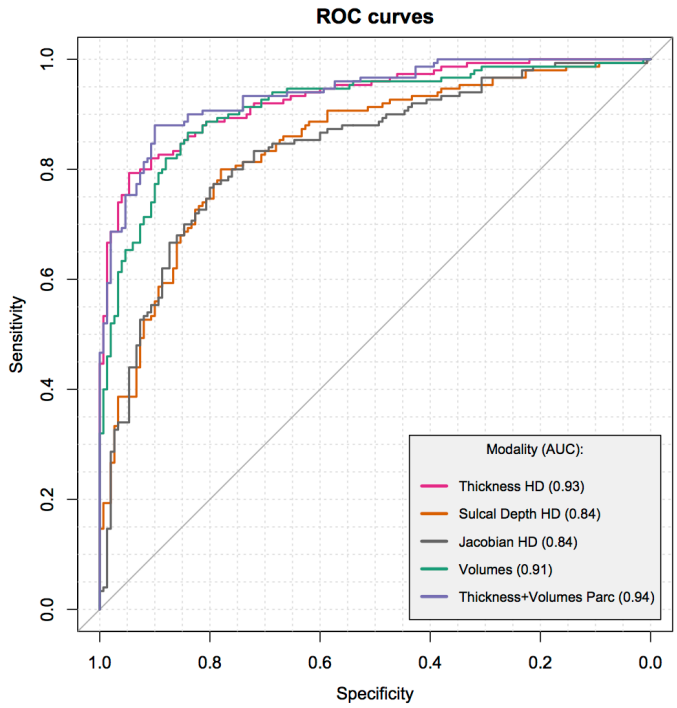

The figure illustrates ROC-curves of the models trained with different morphometric input. Three inputs demonstrate competing performances: high-dimensional (HD) cortical thickness, volumetric data and combined parcellated measurements.
AD/HC – Alzheimer's Disease / Healthy Controls

The best ability to predict MCI-to-AD conversion based on imaging data only was observed for the model in which all RF ensembles were combined by a

majority vote, and was achieved at 76.6% in overall MCI-to-AD conversion detection sensitivity, 2 years before actual dementia onset (averaged value for 6^{th}-, 12^{th}-, 18^{th}- and 24^{th}-month converters) with a specificity of 75.0%.

Adding ApoE genotype and demographics (age, sex, education) as additional predictors into our best AD/HC model, trained using combined cortical thickness and non-cortical volumetric measurements, did not improve AD/HC classification accuracy (*sensitivity/specificity/OA* = 90.7%/82.9%/86.7%). However, its accuracy for MCI-to-AD conversion was significantly higher compared to other models with maximum *sensitivity/specificity/OA* values of 83.3%/81.3%/82.3%. Averaged sensitivity for the first two-year converters was 79.2%.

Robustness in different cohorts

Testing the ADNI models on AddNeuroMed data revealed good generalizability of the classifiers. The best stability (both for AD detection and prediction) was found for the models trained with high-dimensional measures of cortical thickness and parcellated thickness with volumetric measures. Combined models trained using both imaging and non-imaging data demonstrated absence of accuracy drop (see **Table 2.1**).

Table 2.1. Classifiers' performance in the same (ADNI) and separate (AddNeuroMed) cohorts.

Models	AD: Sens/Spec (OA)		MCI-converter 1yr sensitivity*	
	Same cohort (ADNI)	Separate cohort (AddNeuroMed)	Same cohort (ADNI)	Separate cohort (AddNeuroMed)
Thickness	88.6%/90.7% (89.62%)	87%/78% (82.5%)	79.0%	76.2%
Sulcal Depth	80.0%/74.7% (77.3%)	Failed	74.4%	Failed
Jacobian	77.1%/81.3% (79.2%)	78.5%/72% (75.25%)	65.4%	57.1%
Volumes	82.9%/86.7% (84.7%)	70.1%/89% (79.5%)	75.7%	57.1%
Thickness + volumes (parc)	88.6%/92.0% (90.3%)	83.2%/89% (86.1%)	79.0%	71.4%
Morphometry +ApoE +demographics	90.7%/82.9% (86.7%)	84.2%/88.3% (86.25%)	78.0%	79%

The classifiers were trained on the subset from the ADNI dataset and then validated on testing sets from both ADNI (same) and AddNeuroMed (separate) cohorts.
Sens/Spec (OA) – Sensitivity/Specificity (Overall Accuracy);
** – for the AddNeuroMed cohort, definition of the MCI-to-AD converters subgroup (n=21) was defined based on 1-year follow-up.*
NB: We did not compare accuracy to detect MCI non-converters due to only 1-year follow-up available for the AddNeuroMed cohort

Regions of relevance

As expected, the observed pattern of feature relevance was typical for AD and similar in models trained using high-dimensional and parcellated input (**Figures 2.2** and **2.3**. It included atrophy in temporal areas (with more extensive changes

in entorhinal cortex, hippocampus, amygdala), lateral ventricular size differences and parietal cortical abnormalities.

Figure 2.2. Cortical pattern of relevance for Alzheimer's Disease detection: high-dimensional morphometric data.

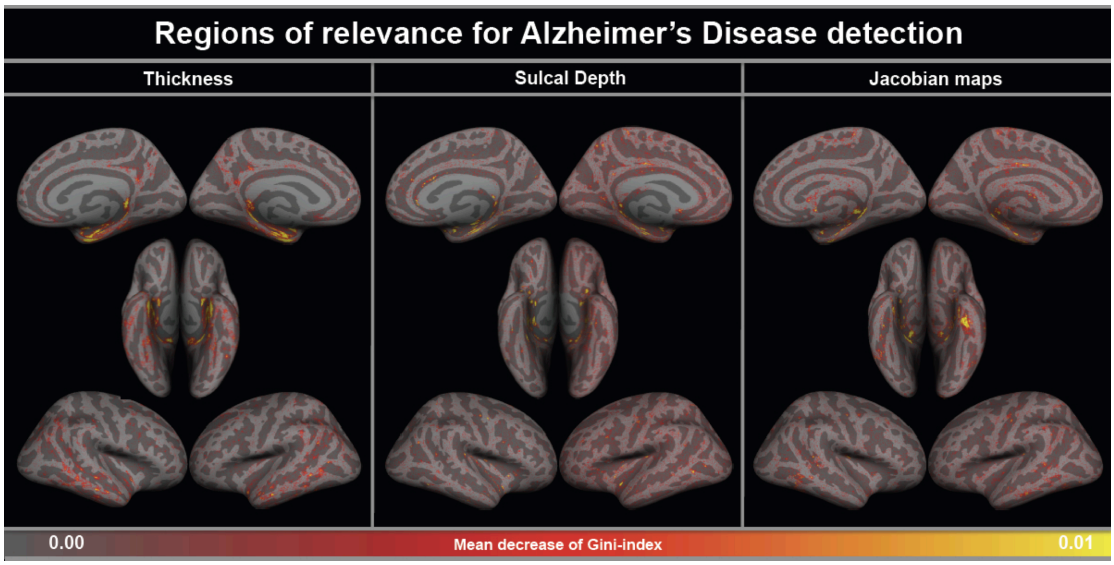

The figure illustrates regions, which were the most relevant for Alzheimer's disease detection based on the mean decrease of the Gini index. In all three high-dimensional modalities, the pattern was AD-specific and included changes predominantly in temporal lobes (with maximum relevance of entorhinal region).

Figure 2.3. Pattern of relevance for Alzheimer's Disease detection: parcellated morphometric data (cortical thickness [DK-atlas] + non-cortical volumes).

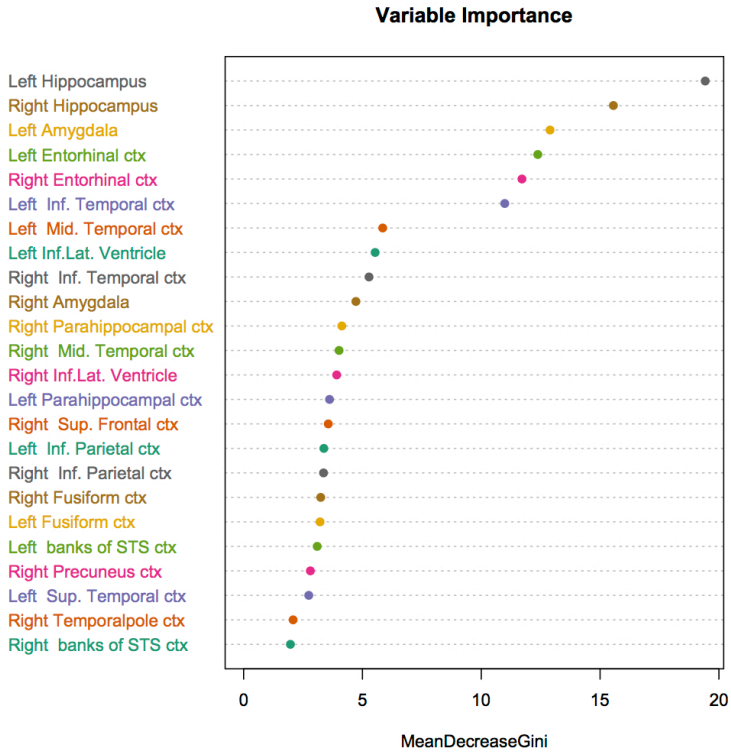

ctx – cortex; Inf. – inferior; Mid. – middle; Sup. – superior;
STS – superior temporal sulcus.
The figure illustrates regions, which were the most relevant for Alzheimer's Disease detection based on the mean decrease of the Gini index. Likewise in the high-dimensional input, the pattern-of-relevance is AD-specific.

5.3 Paper III

Cortical thickness in PD with and without MCI

Mass-univariate analysis revealed cortical thinning in the right inferior temporal gyrus in PD-CN patients compared to healthy controls (**Figure 3.1**).

Comparison of PD-MCI with healthy controls revealed bilateral atrophy in this area, with more prominent thinning in the left hemisphere. Apart from this, PD-MCI patients demonstrated changes in the left superior parietal cortex,

precuneus, lateral occipital, temporal, anterior cingulate and superior frontal areas (**Figure 3.1**).

Compared to PD-CN, PD-MCI patients demonstrated greater thinning in the left precuneus (**Figure 3.1**).

Figure 3.1. Mass-univariate comparison of cortical thickness between A) controls and cognitively normal PD patients (PD-CN), B) controls and PD patients with MCI (PD-MCI) and C) PD-CN and PD-MCI, following the modified PD-MCI-MDS criteria and the PD-MCI-Domains criteria.

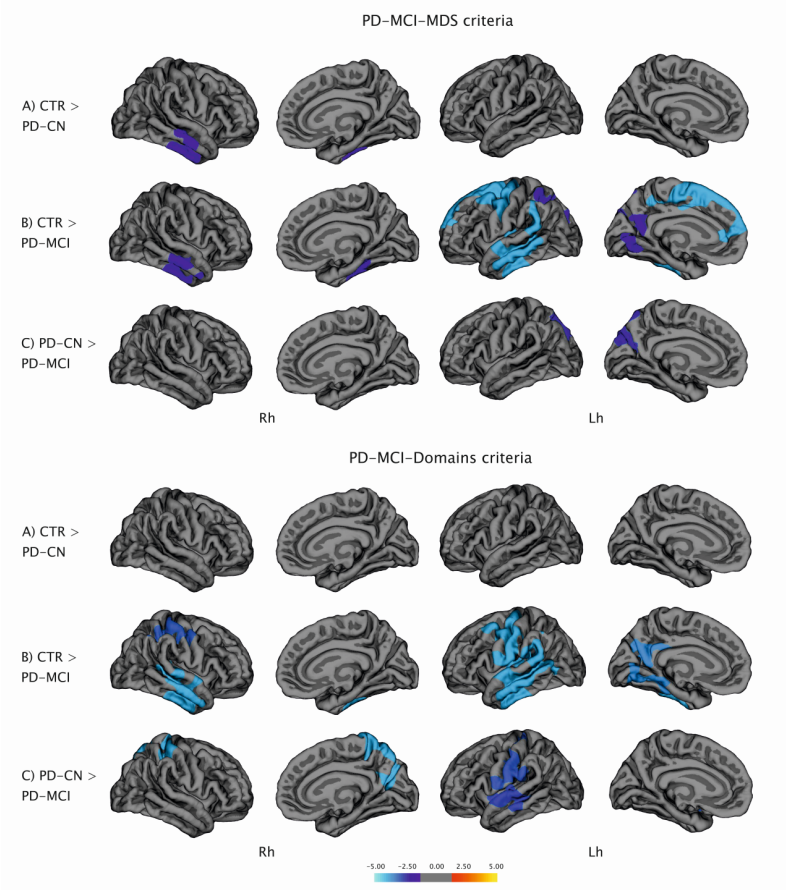

The color scale bar shows the logarithmic scale of p-values ($-log^{10}$). Rh, Right hemisphere; Lh, Left hemisphere.

Cortical thickness and cognitive performance

Results of the analysis of associations between cortical thickness and cognitive domains composite scores are shown in **Figure 3.2**.

Visuospatial performance was associated with superior parietal thickness bilaterally with more extended associations in the right hemisphere (cluster also included the right superior frontal gyrus and precuneus)

The executive domain scores revealed associations with cortical thickness in the superior frontal, precentral, temporal and parietal regions (**Figure 3.2**).

Composite scores of the memory domain did not reveal significant associations with thickness in any cortical area.

Figure 3.2. Mass-univariate GLM analysis of associations between cortical thickness and composite scores in the Visuospatial (A) and Executive (B) cognitive domains in PD patients.

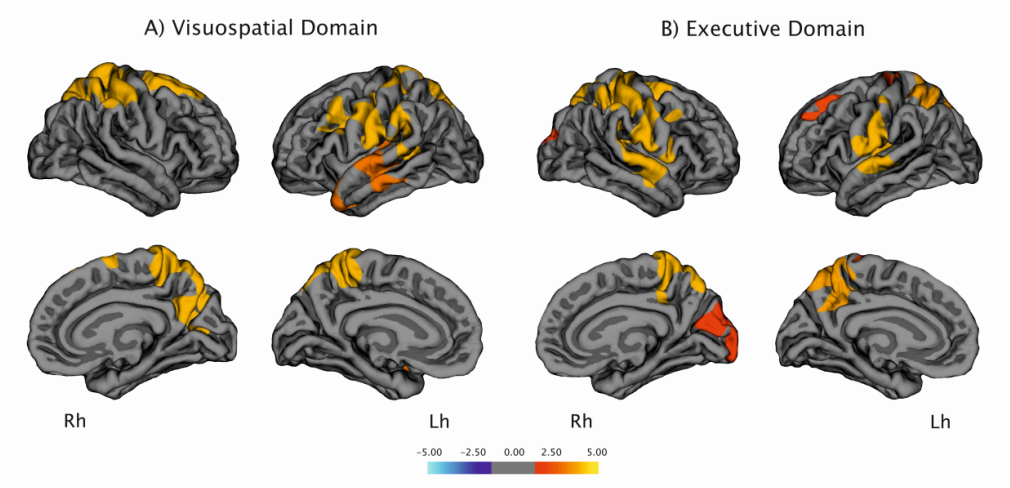

The color scale bar shows the logarithmic scale of p-values (-log10). Rh – Right hemisphere; Lh – Left hemisphere.

5.4 Paper IV

In this study, PLS was used for dimensionality reduction. Each PLS LV score represents one brain-behavior covariance pattern.

Nodal Strength

The first PLS LV represented global effects. Its higher scores were associated with higher strength of all 90 nodes with largest effects on motor, prefrontal cortices and striatum. On a behavioral level, this component was positively associated with motor function (see **Figure 4.1**).

The second LV was associated with higher degree of posterior (supramarginal, superior parietal, posterior cingulate, occipital regions) and striatal nodes, and lower prefronto-limbic (orbitofrontal, anterior cingulate, parahippocampal, temporopolar regions) nodal strength (except for operculo-triangular, middle frontal areas and left hippocampus, which demonstrated positive associations). Behaviorally, this component displayed a negative association with memory function, that is to say that better memory performance was associated with reversed component pattern, favoring the involvement of prefronto-limbic nodes (see **Figure 4.1**).

The third LV, in turn, favored cortical-subcortical segregation with positive associations found in dorsal cortical nodes (dorsolateral prefrontal, frontal and parietal areas) and negative in subcortical structures (hippocampi, striatum, globus pallidus), primary visual, middle temporal and paralimbic (ventral prefrontal) areas. Higher scores of this component were associated with better executive performance (see **Figure 4.1**)

Figure 4.1. Associations between component scores and cognitive functions.

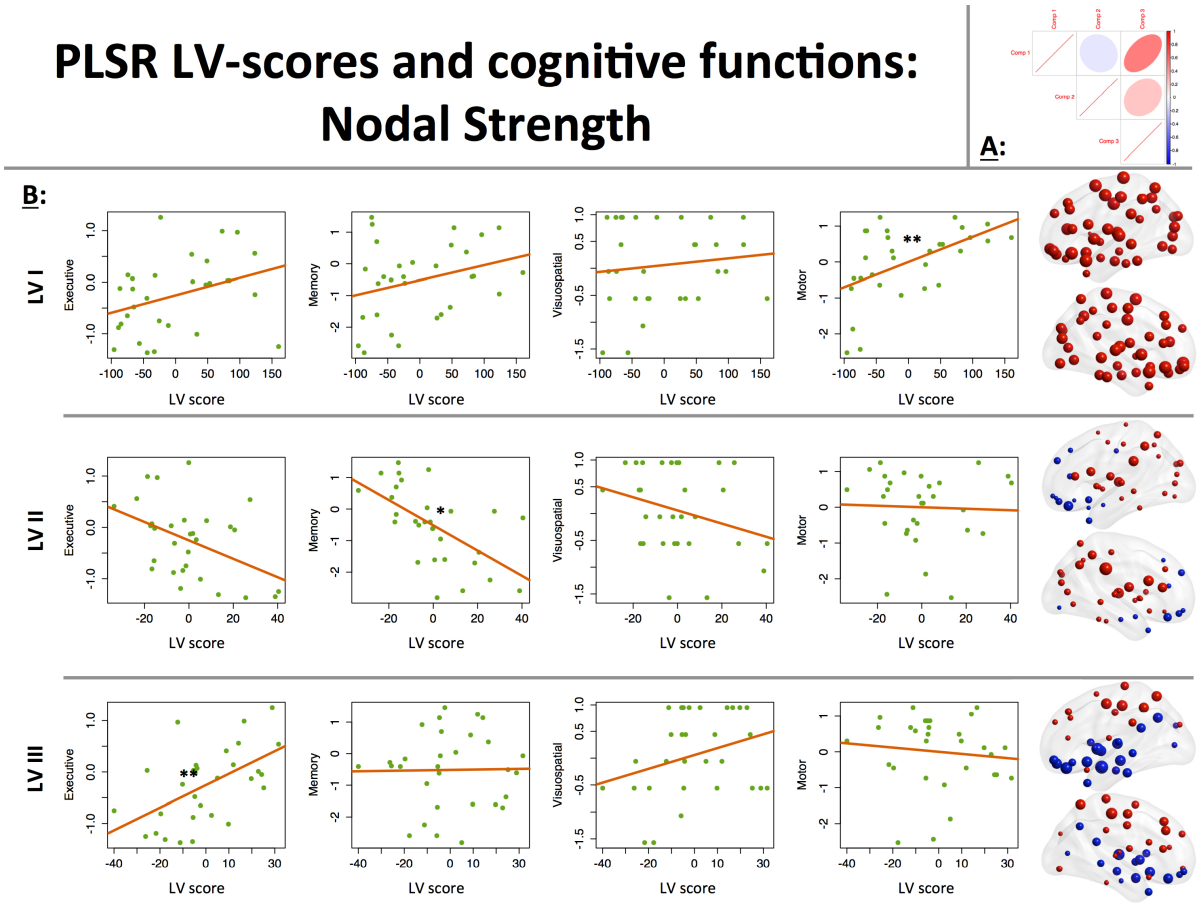

A: Between-component correlation plot. Positive association (r=0.5) was found between latent variables (LVs) I and III.

B: Associations between LV scores extracted from the nodal strength data and performance in 3 cognitive (executive, memory, visuospatial) and motor domains. On the right-hand side of the graph, corresponding loading maps are depicted in brain space, reflecting the relevance of the nodes (spheres) for a particular LV, the magnitude of which is represented by nodal size. Positive loading values are depicted as red spheres, whereas negative ones are shown in blue.

** - $p<0.05$*

*** - $p<0.01$*

Latent Variable scores and caudate DaT uptake

Analysis of the effects of nigrostriatal dopaminergic deficiency on the LVs estimated from the nodal strength revealed significant positive associations of mean caudate SBR ratios with I and III LV-scores (**Figure 4.2**).

This means that higher caudate DaT binding is associated with global increase of nodal strength and segregation toward more active dorsal cortical processing when the subject is at rest.

Figure 4.2. Associations between component scores and mean caudate DaT binding.

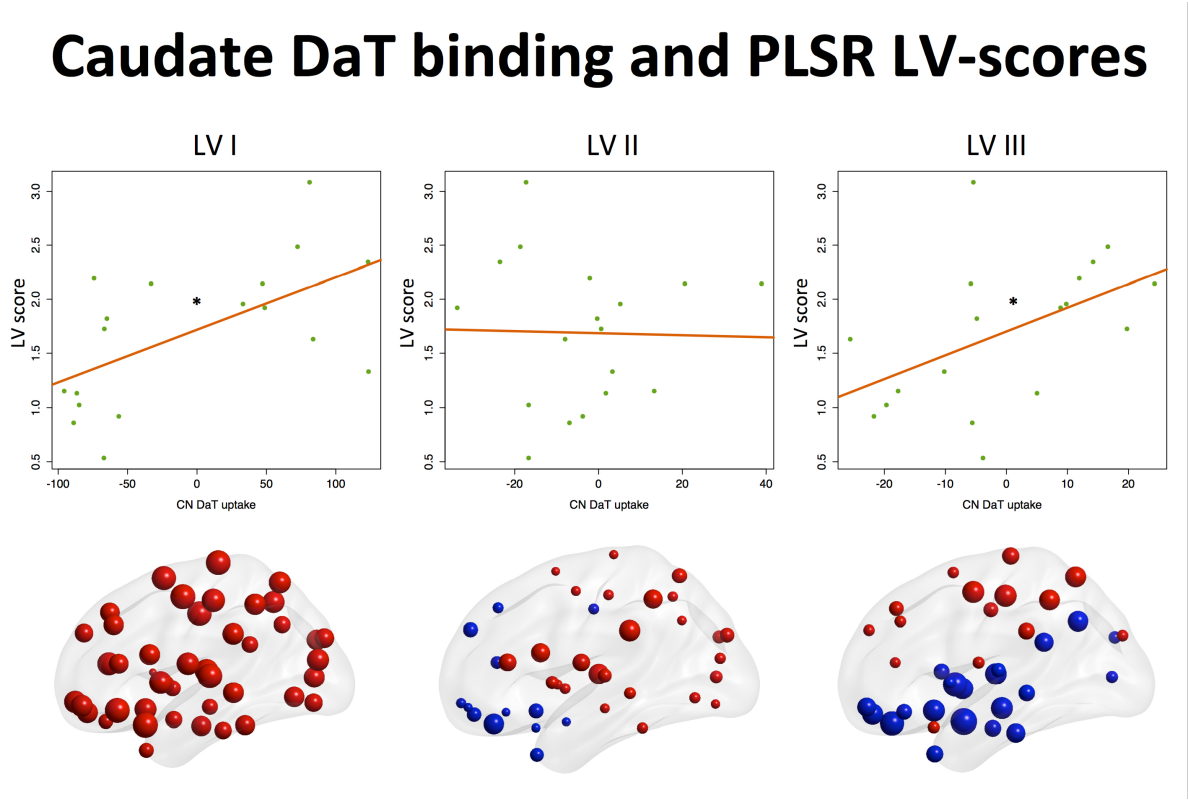

Associations of latent variable (LV) scores extracted from the nodal strength data with nigrostriatal dopaminergic function measured by 123I-FP-CIT SPECT (mean caudate SBR ratios).

Positive associations (- p<0.05) were found for the Ist ("global/motor") and IIIrd ("executive") LVs.*

Corresponding loading maps are depicted in brain space, reflecting the relevance of the nodes (spheres) for a particular LV, the magnitude of which is represented by

nodal size. Positive loading values are depicted as red spheres, whereas negative ones are shown in blue.

Modularity of the cognitive circuitry and caudate DaT uptake

The analysis revealed negative effects of the preserved dopaminergic function on modularity of the cognitive circuit (T = -3.6, 17 DOF, p=0.002), suggesting greater integration among regions within this network (see **Figure 4.3**)

Figure 4.3. Caudate DaT uptake and modularity of the cognitive circuitry at rest.

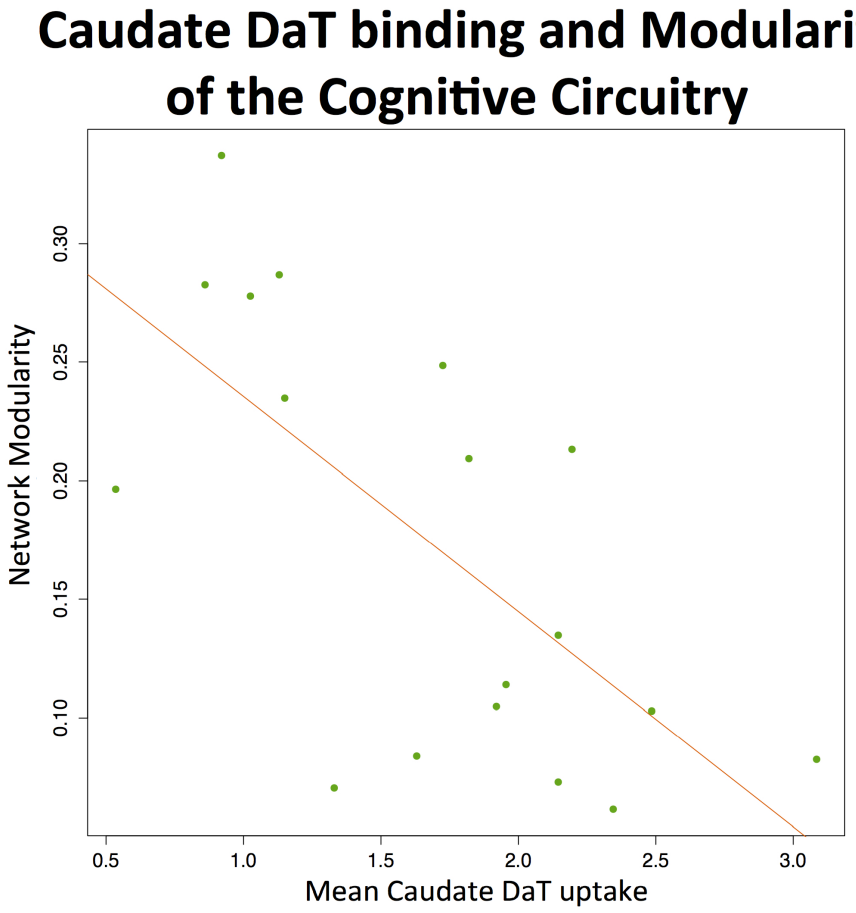

The figure shows significant (p<0.01) negative association between modularity of the cognitive circuitry (identified with automated meta-analysis) and nigrostriatal dopaminergic function measured by 123I-FP-CIT SPECT (mean caudate SBR ratios).

6. Discussion

In this thesis we found that cognitive impairment in the elderly has different brain profiles depending on the predominant neurodegenerative pathology and affected cognitive functions.

Our work is one of the first to demonstrate that with use of pattern recognition techniques applied for MRI data, DLB can be successfully differentiated from AD. This finding was replicated in two independent cohorts (paper I).

The results also suggest that with use of automated computer-aided tools and advanced image processing techniques, Alzheimer's disease can be robustly identified and predicted two years before the actual dementia onset.

Previous studies have successfully employed pattern recognition techniques to classify MRI images from different cohorts only within the combined sets (146). In this thesis we showed that employing our methodology, it is possible to produce classifiers not only with high accuracy, but also with good between-cohort robustness when imaging protocols are carefully aligned (paper II).

We also demonstrated that the accuracy to predict MCI-to-AD conversion (but not AD detection) could be further improved by adding other biomarkers (such as ApoE-genotype) and demographic data. This effect was demonstrated in two completely independent cohorts from North America and Europe (paper II). Further improvement in MCI-to-AD prediction accuracy can potentially be achieved by adding more imaging and non-imaging (i.e., cerebrospinal fluid levels of amyloid-beta, p-tau and t-tau (147)) biomarker modalities and/or by using better image post-processing protocols.

To the best of our knowledge, our work is also the first to investigate the impact of different parcellation schemes and dimensionality of the imaging features on machine learning modelling accuracy, computation/memory and time costs. In the present work (paper II), more disease-specific parcellation scheme (Destrieux's) produced

more accurate models (paper II). Measurement-specific parcellation schemes may also be useful for further accuracy improvement.

Using the largest cohort (to date), our work demonstrated that MCI in PD is associated with temporo-parietal and superior frontal thinning and that memory, visuospatial and executive cognitive performances are related to temporo-parietal and superior frontal thinning (paper III). In contrast to previous studies suggesting that PD without cognitive impairment is not associated with brain atrophy (148, 149), we also found that temporal thinning is present even in PD patients that do not meet criteria for MCI.

On a large-scale network level, better executive performance in PD is associated with increased dorsal fronto-parietal cortical processing and inhibited subcortical and primary sensory involvement when the subject is at resting state. This pattern is positively influenced by the relative preservation of nigrostriatal dopaminergic function (paper IV). In general, higher DaT binding values had integrative effects on the brain (global increase of nodal strength). These findings are in line with previous functional studies employing different methods that revealed abnormally enhanced fronto-subcortical connectivity in PD (87, 150-153)

Influence of nigrostriatal deficiency on brain dynamics underlying PD-related cognitive impairment was also confirmed using global graph theoretical metrics, when higher DaT SBR ratios (relative preservation of dopaminergic function) were associated with lower modularity of cognitive circuitry defined with automated meta-analysis. This is also in line with previous fMRI and magnetoencephalography studies that indicated globally impaired network-level processing in PD (154-156).

The basal ganglia are known to be crucial for sustaining the balance between facilitation and suppression of movements (157). Under certain assumptions, executive functions can be considered as the “movement of thoughts” within this context. According to a widely accepted notion of cognitive cortico-strio-thalamo-cortical loops, DLPFC circuit mediates set-shifting, complex problem-solving, retrieval abilities, organizational strategies, concept-formation, working memory

(158) and other executive functions known to be affected in PD. The nigrostriatal dopamine system therefore may not only allow effective execution/termination of motor activity, but may also assist in smooth switching between cognitive patterns, controlling mutual inhibition and/or facilitation of fronto-subcortical circuits. This is also supported by computational models of the basal ganglia that highlight their routing role in various cognitive functions, particularly for action-selection (159).

Several limitations of our work have to be acknowledged. Nearly all patients were diagnosed clinically, and thus there is a risk for misclassification. This is especially relevant for study I, since DLB and AD can be difficult to differentiate, and mixed Alzheimer's and Lewy body pathology may be present in both AD and DLB groups. However, preliminary post-mortem pathological diagnosis is now available for 21 patients from the DemWest study, and all cases with a clinical diagnosis of probable DLB had cortical or limbic Lewy bodies. In addition, the use of DaTSCAN to confirm the diagnoses of DLB and PD (papers I, III, IV) is a strength that partially overcomes this issue. Another limitation is relatively small sample sizes in the studies I and IV, which may influence feature selection and modeling accuracy. However, the results from study I were replicated in two independent cohorts, and the results of the study IV had high statistical significance and were replicated with two independent approaches using both local (nodal strength) and global metrics (modularity of the cognitive circuitry, defined with meta-analysis). In study III, there is also a potential bias of including "super-normal" controls with MoCA scores > 26, which may artificially increase the difference between PD and control subjects. For the PPMI-based studies (III and IV), there may also be a selection bias due to the fact that the subjects were recruited from highly specialized research centers and might not be representative of a population-based sample. From a methodological standpoint, in study IV, the resting state setting hampers direct interpretation of the findings regarding to the role of brain circuits in the performance of cognitive tasks. Active cognitive processing is associated with patterns of brain dynamics that are different from the ones occurring at rest. These patterns may have different associations with altered dopaminergic function in PD. Another limitation of study IV pertains to the specificity of nigrostriatal dopaminergic deficiency measured by ^{123}I-

FP-CIT SPECT, which might also reflect indirect effects of neurodegeneration of dopaminergic neurons within other pathways (because the severity of dopaminergic deficits may correlate across different systems). Therefore, the results of the study IV should be interpreted with caution. Finally, it is necessary to note that all the cohorts (except for the Slovenian sample) are drawn from the multicenter studies (DemWest, ADNI, AddNeuroMed, PPMI). Within this context, harmonization of clinical and imaging protocols is especially crucial and may represent an issue if not carefully completed. For these studies, cross-center harmonization and reliability assessment steps have been performed using artificial and human phantom scans. Necessity of the harmonization has specifically been demonstrated in the study I, when the model trained on the data from one cohort did not produce appropriate performance on the imaging data acquired without MRI protocol harmonization. However, the model was still effective when trained on the mixed data from non-harmonized cohorts.

Computer-aided framework for the diagnosis of cognitive impairment in clinical practice

Our findings provide a good support for further diagnostic clinical trials of image-based computer-aided models for diagnosis and monitoring of cognitive impairment, particularly for Alzheimer's disease, and suggest that there is a potential of such an implementation for the diagnosis of cognitive impairment associated with PD. Computerized medical decision-support systems is a rapidly developing field with a very strong potential to be used in clinical practice. The results of the present thesis deepen our understanding of brain mechanisms underlying cognitive impairment in the elderly and suggest good implementation feasibility of CAD systems.

However, it is important to note that CAD systems should not be considered as a substitute for a clinician or any other medical specialist. Instead, such a framework implies the use of predictions from computer models as a second opinion that can be taken into account or rejected depending on the clinical context.

In practice, there are many levels at which CAD systems may be beneficial and can be incorporated within the clinical setting (**Figure D-1**).

Figure D-1. Application of CAD in geriatric practice: general scheme.

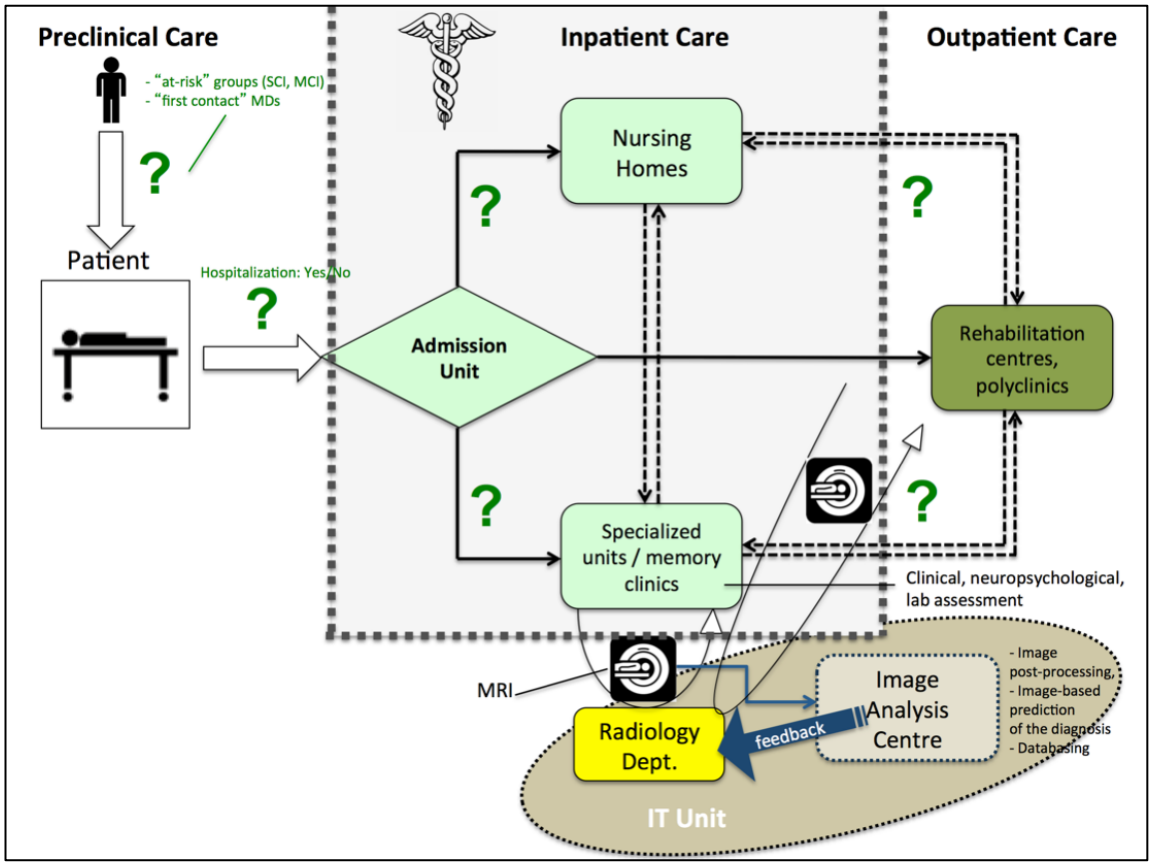

Thus, for example, making a decision on whether a patient with subjective cognitive impairment should be further evaluated, treated or carefully monitored can be substantially augmented with use of CAD. Likewise, such a framework can be used to aid differential diagnosis and prediction of further cognitive decline among patients with early stages of neurodegenerative disease, and finally, to enroll patients at early stages of the diseases to the clinical trials in order to make such interventions most effective and beneficial for the patients.

Nevertheless, it is important to acknowledge that computer-aided medical decision support systems are much more than just optimized pipelines, producing reliable and

accurate models. Instead, such an implementation requires a user-friendly interface easily accessible for a clinician after the specific training is completed.

Clinicians do not necessarily need to participate in the image preprocessing at any stage except for probably general image quality control step. An ideal CAD system of this kind would be software with “point-and-click” interface that would take DICOM images as an input and produce the required measures and predictions as an output.

Incorporating this is not an easy task to accomplish for several reasons. First of all, image-processing packages are being constantly updated improving quality and efficiency of the data preparation step. This, in turn, influences prediction accuracy of the models and not always towards its improvement. Pattern recognition algorithms and their implementations are also being optimized in the newest version of the toolboxes. All of the above requires flexible and modifiable implementation, as well as coordinated work of several IT and medical specialists. On the other hand, there is a well-known tradeoff between functionality/capability on the one side and complexity/cost on the other. Therefore, every update of the software should be standalone and non-modifiable for the clinical users.

Another important issue pertains to the clinical setting itself, within which information about patients and clinical details including the diagnosis itself can be changed after a while. Within the context of continuous image data and clinical information flow it would be beneficial to incorporate so-called “online” machine learning setting, where the model gradually "learns" using one instance at a time (instead of traditional "offline" or “batch” learning framework, where the whole training set is available to the algorithm at the beginning and therefore does not allow any modifications of the models after the training has been completed).

This framework also provides valid estimations of the prediction confidence under a general i.i.d. assumption (independent and identically distributed) (160-162).

Since this approach can be applied to an individual patient and gives reliable estimations of possible diagnoses, it has strong potential to be used in clinical practice

and, to our opinion, would be the best candidate for diagnostic trials employing computer-aided medical decision-support systems.

There are also many important organizational issues pertaining to the implementation of CAD system in clinical practice, which were beyond the scope of the thesis, such as incentives for clinicians and practicalities related to data transfer and patients' confidentiality. These issues are relevant for any IT innovations in medicine and can be effectively addressed as well.

7. Conclusions

Cognitive impairment in the elderly has different brain profiles depending on the predominant neurodegenerative pathology and cognitive functions affected. With the use of automated computer-aided tools and advanced image processing techniques, Alzheimer's disease can be robustly identified, predicted two years before the actual dementia onset and differentiated from dementia with Lewy bodies. After certain modifications and adaptations for clinicians, the models can be successfully incorporated into medical decision-support systems and be evaluated in subsequent diagnostic clinical trials.

The identified brain structural and functional profile associated with Parkinson's-related cognitive impairment is also robust and, holding strong diagnostic potential, must be detectable using computer-aided systems of similar design, the development of which is the matter of our future research. The development and future elaboration of clinically realistic computer-aided systems for the diagnosis of neurodegenerative diseases is an important topic for future research.

8. References

1. McKeith IG, Dickson DW, Lowe J, Emre M, O'Brien JT, Feldman H, et al. Diagnosis and management of dementia with Lewy bodies: third report of the DLB Consortium. Neurology. 2005;65(12):1863-72.
2. Oxford Dictionaries: "Cognition". LINK: http://www.oxforddictionaries.com/definition/english/cognition.
3. Taylor L. E-Learning MOOC BLOG: The Cognitive Revolution. LINK: http://louisecharente.wordpress.com/2013/08/21/the-cognitive-revolution/. Worldpress; 2013 [cited 2014 January 2014].
4. Kravitz E, Schmeidler J, Beeri MS. Cognitive decline and dementia in the oldest-old. Rambam Maimonides Med J. 2012;3(4):e0026.
5. Hjort PF, Waaler HT. [Dementia towards 2050]. Tidsskr Nor Laegeforen. 2010;130(13):1356-8.
6. Hurd MD, Martorell P, Delavande A, Mullen KJ, Langa KM. Monetary costs of dementia in the United States. N Engl J Med. 2013;368(14):1326-34.
7. Alzheimer's Disease International (ADI). World Alzheimer Report 2010: The Global Economic Impact of Dementia. URL: http://www.alz.co.uk/research/files/WorldAlzheimerReport2010.pdf.
8. American Geriatrics Society. "The Demand for Geriatric Care and the Evident Shortage of Geriatrics Healthcare Providers." http://www.americangeriatrics.org/files/documents/Adv_Resources/demand_for_geriatric_care.pdf March 2013.
9. Alzheimer's Disease International (ADI). World Alzheimer Report 2011: The Global Economic Impact of Dementia. URL: http://www.alz.co.uk/research/WorldAlzheimerReport2011.pdf.
10. Barkhof F, Fox NC, Bastos-Leite AJ, Scheltens P. Neuroimaging in Dementia. 1st Edition ed: Springer; 2011.
11. Lauterbur PC. Image formation by induced local interactions. Examples employing nuclear magnetic resonance. . Clin Orthop Relat Res. 1973(244):3-6.
12. O'Brien JT. Role of imaging techniques in the diagnosis of dementia. Br J Radiol. 2007;80 Spec No 2:S71-7.
13. Modo M, Bulte JWM. Magnetic Resonance Neuroimaging: Materials and Protocols: Humana Press; 2011.
14. Dubois B, Feldman HH, Jacova C, Dekosky ST, Barberger-Gateau P, Cummings J, et al. Research criteria for the diagnosis of Alzheimer's disease: revising the NINCDS-ADRDA criteria. Lancet Neurol. 2007;6(8):734-46.
15. O'Donovan J, Watson R, Colloby SJ, Firbank MJ, Burton EJ, Barber R, et al. Does posterior cortical atrophy on MRI discriminate between Alzheimer's disease, dementia with Lewy bodies, and normal aging? Int Psychogeriatr. 2013;25(1):111-9.
16. Pantel J, Schonknecht P, Essig M, Schroder J. Distribution of cerebral atrophy assessed by magnetic resonance imaging reflects patterns of neuropsychological deficits in Alzheimer's dementia. Neurosci Lett. 2004;361(1-3):17-20.
17. Shim YS, Youn YC, Na DL, Kim SY, Cheong HK, Moon SY, et al. Effects of medial temporal atrophy and white matter hyperintensities on the cognitive functions in patients with Alzheimer's disease. Eur Neurol. 2011;66(2):75-82.
18. Smits LL, Tijms BM, Benedictus MR, Koedam EL, Koene T, Reuling IE, et al. Regional atrophy is associated with impairment in distinct cognitive domains in Alzheimer's disease. Alzheimers Dement. 2013.

19. Dickerson BC, Wolk DA, Alzheimer's Disease Neuroimaging I. Dysexecutive versus amnesic phenotypes of very mild Alzheimer's disease are associated with distinct clinical, genetic and cortical thinning characteristics. J Neurol Neurosurg Psychiatry. 2011;82(1):45-51.
20. Murray ME, Graff-Radford NR, Ross OA, Petersen RC, Duara R, Dickson DW. Neuropathologically defined subtypes of Alzheimer's disease with distinct clinical characteristics: a retrospective study. Lancet Neurol. 2011;10(9):785-96.
21. Whitwell JL, Dickson DW, Murray ME, Weigand SD, Tosakulwong N, Senjem ML, et al. Neuroimaging correlates of pathologically defined subtypes of Alzheimer's disease: a case-control study. Lancet Neurol. 2012;11(10):868-77.
22. Whitwell JL, Jack CR, Jr., Przybelski SA, Parisi JE, Senjem ML, Boeve BF, et al. Temporoparietal atrophy: a marker of AD pathology independent of clinical diagnosis. Neurobiol Aging. 2011;32(9):1531-41.
23. Ridgway GR, Lehmann M, Barnes J, Rohrer JD, Warren JD, Crutch SJ, et al. Early-onset Alzheimer disease clinical variants: multivariate analyses of cortical thickness. Neurology. 2012;79(1):80-4.
24. Frisoni GB, Pievani M, Testa C, Sabattoli F, Bresciani L, Bonetti M, et al. The topography of grey matter involvement in early and late onset Alzheimer's disease. Brain. 2007;130(Pt 3):720-30.
25. Koedam EL, Lauffer V, van der Vlies AE, van der Flier WM, Scheltens P, Pijnenburg YA. Early-versus late-onset Alzheimer's disease: more than age alone. J Alzheimers Dis. 2010;19(4):1401-8.
26. Ewers M, Frisoni GB, Teipel SJ, Grinberg LT, Amaro E, Jr., Heinsen H, et al. Staging Alzheimer's disease progression with multimodality neuroimaging. Prog Neurobiol. 2011;95(4):535-46.
27. Scheltens P, Leys D, Barkhof F, Huglo D, Weinstein HC, Vermersch P, et al. Atrophy of medial temporal lobes on MRI in "probable" Alzheimer's disease and normal ageing: diagnostic value and neuropsychological correlates. J Neurol Neurosurg Psychiatry. 1992;55(10):967-72.
28. Duara R, Loewenstein DA, Potter E, Appel J, Greig MT, Urs R, et al. Medial temporal lobe atrophy on MRI scans and the diagnosis of Alzheimer disease. Neurology. 2008;71(24):1986-92.
29. Burton EJ, Barber R, Mukaetova-Ladinska EB, Robson J, Perry RH, Jaros E, et al. Medial temporal lobe atrophy on MRI differentiates Alzheimer's disease from dementia with Lewy bodies and vascular cognitive impairment: a prospective study with pathological verification of diagnosis. Brain. 2009;132(Pt 1):195-203.
30. Korf ES, Wahlund LO, Visser PJ, Scheltens P. Medial temporal lobe atrophy on MRI predicts dementia in patients with mild cognitive impairment. Neurology. 2004;63(1):94-100.
31. DeCarli C, Frisoni GB, Clark CM, Harvey D, Grundman M, Petersen RC, et al. Qualitative estimates of medial temporal atrophy as a predictor of progression from mild cognitive impairment to dementia. Arch Neurol. 2007;64(1):108-15.
32. Vemuri P, Simon G, Kantarci K, Whitwell JL, Senjem ML, Przybelski SA, et al. Antemortem differential diagnosis of dementia pathology using structural MRI: Differential-STAND. Neuroimage. 2011;55(2):522-31.
33. Kwong KK, Belliveau JW, Chesler DA, Goldberg IE, Weisskoff RM, Poncelet BP, et al. Dynamic magnetic resonance imaging of human brain activity during primary sensory stimulation. Proc Natl Acad Sci U S A. 1992;89(12):5675-9.

34. Fox MD, Snyder AZ, Vincent JL, Corbetta M, Van Essen DC, Raichle ME. The human brain is intrinsically organized into dynamic, anticorrelated functional networks. Proc Natl Acad Sci U S A. 2005;102(27):9673-8.
35. Galvin JE, Price JL, Yan Z, Morris JC, Sheline YI. Resting bold fMRI differentiates dementia with Lewy bodies vs Alzheimer disease. Neurology. 2011;76(21):1797-803.
36. Barber R, McKeith IG, Ballard C, Gholkar A, O'Brien JT. A comparison of medial and lateral temporal lobe atrophy in dementia with Lewy bodies and Alzheimer's disease: magnetic resonance imaging volumetric study. Dement Geriatr Cogn Disord. 2001;12(3):198-205.
37. McKeith IG, Galasko D, Kosaka K, Perry EK, Dickson DW, Hansen LA, et al. Consensus guidelines for the clinical and pathologic diagnosis of dementia with Lewy bodies (DLB): report of the consortium on DLB international workshop. Neurology. 1996;47(5):1113-24.
38. McKeith I, Mintzer J, Aarsland D, Burn D, Chiu H, Cohen-Mansfield J, et al. Dementia with Lewy bodies. Lancet Neurol. 2004;3(1):19-28.
39. Calderon J, Perry RJ, Erzinclioglu SW, Berrios GE, Dening TR, Hodges JR. Perception, attention, and working memory are disproportionately impaired in dementia with Lewy bodies compared with Alzheimer's disease. J Neurol Neurosurg Psychiatry. 2001;70(2):157-64.
40. Simard M, van Reekum R, Myran D. Visuospatial impairment in dementia with Lewy bodies and Alzheimer's disease: a process analysis approach. Int J Geriatr Psychiatry. 2003;18(5):387-91.
41. Noe E, Marder K, Bell KL, Jacobs DM, Manly JJ, Stern Y. Comparison of dementia with Lewy bodies to Alzheimer's disease and Parkinson's disease with dementia. Mov Disord. 2004;19(1):60-7.
42. Park KW, Kim HS, Cheon SM, Cha JK, Kim SH, Kim JW. Dementia with Lewy Bodies versus Alzheimer's Disease and Parkinson's Disease Dementia: A Comparison of Cognitive Profiles. J Clin Neurol. 2011;7(1):19-24.
43. Kovari E, Gold G, Herrmann FR, Canuto A, Hof PR, Bouras C, et al. Lewy body densities in the entorhinal and anterior cingulate cortex predict cognitive deficits in Parkinson's disease. Acta Neuropathol. 2003;106(1):83-8.
44. Colloby SJ, Fenwick JD, Williams ED, Paling SM, Lobotesis K, Ballard C, et al. A comparison of (99m)Tc-HMPAO SPET changes in dementia with Lewy bodies and Alzheimer's disease using statistical parametric mapping. Eur J Nucl Med Mol Imaging. 2002;29(5):615-22.
45. Gomperts SN, Rentz DM, Moran E, Becker JA, Locascio JJ, Klunk WE, et al. Imaging amyloid deposition in Lewy body diseases. Neurology. 2008;71(12):903-10.
46. Firbank MJ, Blamire AM, Krishnan MS, Teodorczuk A, English P, Gholkar A, et al. Atrophy is associated with posterior cingulate white matter disruption in dementia with Lewy bodies and Alzheimer's disease. Neuroimage. 2007;36(1):1-7.
47. Kamagata K, Motoi Y, Abe O, Shimoji K, Hori M, Nakanishi A, et al. White matter alteration of the cingulum in Parkinson disease with and without dementia: evaluation by diffusion tensor tract-specific analysis. AJNR Am J Neuroradiol. 2012;33(5):890-5.
48. Burton EJ, Karas G, Paling SM, Barber R, Williams ED, Ballard CG, et al. Patterns of cerebral atrophy in dementia with Lewy bodies using voxel-based morphometry. Neuroimage. 2002;17(2):618-30.
49. Burton EJ, McKeith IG, Burn DJ, Williams ED, O'Brien JT. Cerebral atrophy in Parkinson's disease with and without dementia: a comparison with Alzheimer's disease, dementia with Lewy bodies and controls. Brain. 2004;127(Pt 4):791-800.

50. Brenneis C, Wenning GK, Egger KE, Schocke M, Trieb T, Seppi K, et al. Basal forebrain atrophy is a distinctive pattern in dementia with Lewy bodies. Neuroreport. 2004;15(11):1711-4.
51. Ballmaier M, O'Brien JT, Burton EJ, Thompson PM, Rex DE, Narr KL, et al. Comparing gray matter loss profiles between dementia with Lewy bodies and Alzheimer's disease using cortical pattern matching: diagnosis and gender effects. Neuroimage. 2004;23(1):325-35.
52. Whitwell JL, Weigand SD, Shiung MM, Boeve BF, Ferman TJ, Smith GE, et al. Focal atrophy in dementia with Lewy bodies on MRI: a distinct pattern from Alzheimer's disease. Brain. 2007;130(Pt 3):708-19.
53. Minoshima S, Foster NL, Sima AA, Frey KA, Albin RL, Kuhl DE. Alzheimer's disease versus dementia with Lewy bodies: cerebral metabolic distinction with autopsy confirmation. Ann Neurol. 2001;50(3):358-65.
54. Hanyu H, Shimizu S, Hirao K, Kanetaka H, Sakurai H, Iwamoto T, et al. Differentiation of dementia with Lewy bodies from Alzheimer's disease using Mini-Mental State Examination and brain perfusion SPECT. J Neurol Sci. 2006;250(1-2):97-102.
55. Middelkoop HA, van der Flier WM, Burton EJ, Lloyd AJ, Paling S, Barber R, et al. Dementia with Lewy bodies and AD are not associated with occipital lobe atrophy on MRI. Neurology. 2001;57(11):2117-20.
56. Ishii K, Soma T, Kono AK, Sofue K, Miyamoto N, Yoshikawa T, et al. Comparison of regional brain volume and glucose metabolism between patients with mild dementia with lewy bodies and those with mild Alzheimer's disease. J Nucl Med. 2007;48(5):704-11.
57. Muslimovic D, Post B, Speelman JD, Schmand B. Cognitive profile of patients with newly diagnosed Parkinson disease. Neurology. 2005;65(8):1239-45.
58. Vossius C, Larsen JP, Janvin C, Aarsland D. The economic impact of cognitive impairment in Parkinson's disease. Mov Disord. 2011;26(8):1541-4.
59. Svenningsson P, Westman E, Ballard C, Aarsland D. Cognitive impairment in patients with Parkinson's disease: diagnosis, biomarkers, and treatment. Lancet Neurol. 2012;11(8):697-707.
60. Aarsland D, Bronnick K, Larsen JP, Tysnes OB, Alves G, Norwegian ParkWest Study G. Cognitive impairment in incident, untreated Parkinson disease: the Norwegian ParkWest study. Neurology. 2009;72(13):1121-6.
61. Williams-Gray CH, Evans JR, Goris A, Foltynie T, Ban M, Robbins TW, et al. The distinct cognitive syndromes of Parkinson's disease: 5 year follow-up of the CamPaIGN cohort. Brain. 2009;132(Pt 11):2958-69.
62. Aarsland D, Andersen K, Larsen JP, Lolk A, Kragh-Sorensen P. Prevalence and characteristics of dementia in Parkinson disease: an 8-year prospective study. Arch Neurol. 2003;60(3):387-92.
63. Narayanan NS, Rodnitzky RL, Uc EY. Prefrontal dopamine signaling and cognitive symptoms of Parkinson's disease. Rev Neurosci. 2013;24(3):267-78.
64. Hirano S, Shinotoh H, Eidelberg D. Functional brain imaging of cognitive dysfunction in Parkinson's disease. J Neurol Neurosurg Psychiatry. 2012;83(10):963-9.
65. Christopher L, Strafella AP. Neuroimaging of brain changes associated with cognitive impairment in Parkinson's disease. J Neuropsychol. 2013;7(2):225-40.
66. Ito K, Nagano-Saito A, Kato T, Arahata Y, Nakamura A, Kawasumi Y, et al. Striatal and extrastriatal dysfunction in Parkinson's disease with dementia: a 6-[18F]fluoro-L-dopa PET study. Brain. 2002;125(Pt 6):1358-65.
67. O'Brien JT, Colloby S, Fenwick J, Williams ED, Firbank M, Burn D, et al. Dopamine transporter loss visualized with FP-CIT SPECT in the differential diagnosis of dementia with Lewy bodies. Arch Neurol. 2004;61(6):919-25.

68. Bruck A, Portin R, Lindell A, Laihinen A, Bergman J, Haaparanta M, et al. Positron emission tomography shows that impaired frontal lobe functioning in Parkinson's disease is related to dopaminergic hypofunction in the caudate nucleus. Neurosci Lett. 2001;311(2):81-4.
69. Cheesman AL, Barker RA, Lewis SJ, Robbins TW, Owen AM, Brooks DJ. Lateralisation of striatal function: evidence from 18F-dopa PET in Parkinson's disease. J Neurol Neurosurg Psychiatry. 2005;76(9):1204-10.
70. Cropley VL, Fujita M, Bara-Jimenez W, Brown AK, Zhang XY, Sangare J, et al. Pre- and post-synaptic dopamine imaging and its relation with frontostriatal cognitive function in Parkinson disease: PET studies with [11C]NNC 112 and [18F]FDOPA. Psychiatry Res. 2008;163(2):171-82.
71. Mentis MJ, McIntosh AR, Perrine K, Dhawan V, Berlin B, Feigin A, et al. Relationships among the metabolic patterns that correlate with mnemonic, visuospatial, and mood symptoms in Parkinson's disease. Am J Psychiatry. 2002;159(5):746-54.
72. Huang C, Mattis P, Tang C, Perrine K, Carbon M, Eidelberg D. Metabolic brain networks associated with cognitive function in Parkinson's disease. Neuroimage. 2007;34(2):714-23.
73. Huang C, Tang C, Feigin A, Lesser M, Ma Y, Pourfar M, et al. Changes in network activity with the progression of Parkinson's disease. Brain. 2007;130(Pt 7):1834-46.
74. Eidelberg D. Metabolic brain networks in neurodegenerative disorders: a functional imaging approach. Trends Neurosci. 2009;32(10):548-57.
75. Owen AM, Doyon J, Dagher A, Sadikot A, Evans AC. Abnormal basal ganglia outflow in Parkinson's disease identified with PET. Implications for higher cortical functions. Brain. 1998;121 (Pt 5):949-65.
76. Dagher A, Owen AM, Boecker H, Brooks DJ. The role of the striatum and hippocampus in planning: a PET activation study in Parkinson's disease. Brain. 2001;124(Pt 5):1020-32.
77. Cools R, Stefanova E, Barker RA, Robbins TW, Owen AM. Dopaminergic modulation of high-level cognition in Parkinson's disease: the role of the prefrontal cortex revealed by PET. Brain. 2002;125(Pt 3):584-94.
78. Lewis SJ, Dove A, Robbins TW, Barker RA, Owen AM. Cognitive impairments in early Parkinson's disease are accompanied by reductions in activity in frontostriatal neural circuitry. J Neurosci. 2003;23(15):6351-6.
79. Ekman U, Eriksson J, Forsgren L, Mo SJ, Riklund K, Nyberg L. Functional brain activity and presynaptic dopamine uptake in patients with Parkinson's disease and mild cognitive impairment: a cross-sectional study. Lancet Neurol. 2012;11(8):679-87.
80. Mattay VS, Tessitore A, Callicott JH, Bertolino A, Goldberg TE, Chase TN, et al. Dopaminergic modulation of cortical function in patients with Parkinson's disease. Ann Neurol. 2002;51(2):156-64.
81. Monchi O, Petrides M, Doyon J, Postuma RB, Worsley K, Dagher A. Neural bases of set-shifting deficits in Parkinson's disease. J Neurosci. 2004;24(3):702-10.
82. Monchi O, Petrides M, Mejia-Constain B, Strafella AP. Cortical activity in Parkinson's disease during executive processing depends on striatal involvement. Brain. 2007;130(Pt 1):233-44.
83. Tinaz S, Schendan HE, Stern CE. Fronto-striatal deficit in Parkinson's disease during semantic event sequencing. Neurobiol Aging. 2008;29(3):397-407.
84. van Eimeren T, Monchi O, Ballanger B, Strafella AP. Dysfunction of the default mode network in Parkinson disease: a functional magnetic resonance imaging study. Arch Neurol. 2009;66(7):877-83.

85. Wu T, Wang L, Chen Y, Zhao C, Li K, Chan P. Changes of functional connectivity of the motor network in the resting state in Parkinson's disease. Neurosci Lett. 2009;460(1):6-10.
86. Helmich RC, Derikx LC, Bakker M, Scheeringa R, Bloem BR, Toni I. Spatial remapping of cortico-striatal connectivity in Parkinson's disease. Cereb Cortex. 2010;20(5):1175-86.
87. Kwak Y, Peltier S, Bohnen NI, Muller ML, Dayalu P, Seidler RD. Altered resting state cortico-striatal connectivity in mild to moderate stage Parkinson's disease. Front Syst Neurosci. 2010;4:143.
88. Esposito F, Tessitore A, Giordano A, De Micco R, Paccone A, Conforti R, et al. Rhythm-specific modulation of the sensorimotor network in drug-naive patients with Parkinson's disease by levodopa. Brain. 2013;136(Pt 3):710-25.
89. Thompson PM, Apostolova LG. Computational anatomical methods as applied to ageing and dementia. Br J Radiol. 2007;80 Spec No 2:S78-91.
90. Gray KR, Aljabar P, Heckemann RA, Hammers A, Rueckert D, Alzheimer's Disease Neuroimaging I. Random forest-based similarity measures for multi-modal classification of Alzheimer's disease. Neuroimage. 2013;65:167-75.
91. Liu M, Zhang D, Shen D, Alzheimer's Disease Neuroimaging I. Ensemble sparse classification of Alzheimer's disease. Neuroimage. 2012;60(2):1106-16.
92. Cuingnet R, Gerardin E, Tessieras J, Auzias G, Lehericy S, Habert MO, et al. Automatic classification of patients with Alzheimer's disease from structural MRI: a comparison of ten methods using the ADNI database. Neuroimage. 2011;56(2):766-81.
93. Kloppel S, Stonnington CM, Chu C, Draganski B, Scahill RI, Rohrer JD, et al. Automatic classification of MR scans in Alzheimer's disease. Brain. 2008;131(Pt 3):681-9.
94. Stoitsis J, Valavanis I, Mougiakakou SG, Golemati S, Nikita A, Nikita KS.

Computer aided diagnosis based on medical image processing and artificial intelligence methods. Nuclear Instruments and Methods in Physics 2006(Research A 569): 591-5.
95. Flanagan ME, Saleem JJ, Millitello LG, Russ AL, Doebbeling BN. Paper- and computer-based workarounds to electronic health record use at three benchmark institutions. J Am Med Inform Assoc. 2013;Published Online First.
96. Simborg DW, Detmer DE, Berner ES. The wave has finally broken: now what? J Am Med Inform Assoc. 2013;Published Online First.
97. Terry K. Doctors Are Increasingly Dissatisfied With EHRs. 29.04.2013 [cited 2013]; Available from: http://www.ihealthbeat.org/features/2013/doctors-are-increasingly-dissatisfied-with-ehrs.aspx.
98. Emre M. Cognitive Impairment and Dementia in Parkinson's Disease: Oxford University Press; 2010.
99. Aarsland D, Rongve A, Nore SP, Skogseth R, Skulstad S, Ehrt U, et al. Frequency and case identification of dementia with Lewy bodies using the revised consensus criteria. Dement Geriatr Cogn Disord. 2008;26(5):445-52.
100. Rizopoulos D. ltm: An R package for Latent Variable Modelling and Item Response Theory Analyses. Journal of Statistical Software. 2006;17 (5):1-25.
101. R Core Team (2012). R: A language and environment for statistical computing. R Foundation for Statistical Computing, Vienna, Austria. ISBN: 3-900051-07-0. URL: http://www.R-project.org/.
102. McKhann G, Drachman D, Folstein M, Katzman R, Price D, Stadlan EM. Clinical diagnosis of Alzheimer's disease: report of the NINCDS-ADRDA Work Group under the auspices of Department of Health and Human Services Task Force on Alzheimer's Disease. Neurology. 1984;34(7):939-44.

103. Emre M, Aarsland D, Brown R, Burn DJ, Duyckaerts C, Mizuno Y, et al. Clinical diagnostic criteria for dementia associated with Parkinson's disease. Mov Disord. 2007;22(12):1689-707; quiz 837.
104. Lippa CF, Duda JE, Grossman M, Hurtig HI, Aarsland D, Boeve BF, et al. DLB and PDD boundary issues: diagnosis, treatment, molecular pathology, and biomarkers. Neurology. 2007;68(11):812-9.
105. Simmons A, Westman E, Muehlboeck S, Mecocci P, Vellas B, Tsolaki M, et al. The AddNeuroMed framework for multi-centre MRI assessment of Alzheimer's disease: experience from the first 24 months. Int J Geriatr Psychiatry. 2011;26(1):75-82.
106. Parkinson Progression Marker I. The Parkinson Progression Marker Initiative (PPMI). Prog Neurobiol. 2011;95(4):629-35.
107. Benton AL, Varney NR, Hamsher KD. Visuospatial judgment. A clinical test. Arch Neurol. 1978;35(6):364-7.
108. Shapiro AM, Benedict RH, Schretlen D, Brandt J. Construct and concurrent validity of the Hopkins Verbal Learning Test-revised. Clin Neuropsychol. 1999;13(3):348-58.
109. Litvan I, Goldman JG, Troster AI, Schmand BA, Weintraub D, Petersen RC, et al. Diagnostic criteria for mild cognitive impairment in Parkinson's disease: Movement Disorder Society Task Force guidelines. Mov Disord. 2012;27(3):349-56.
110. Dubois B, Burn D, Goetz C, Aarsland D, Brown RG, Broe GA, et al. Diagnostic procedures for Parkinson's disease dementia: recommendations from the movement disorder society task force. Mov Disord. 2007;22(16):2314-24.
111. Booij J, Hemelaar TG, Speelman JD, de Bruin K, Janssen AG, van Royen EA. One-day protocol for imaging of the nigrostriatal dopaminergic pathway in Parkinson's disease by [123I]FPCIT SPECT. J Nucl Med. 1999;40(5):753-61.
112. Dale AM, Fischl B, Sereno MI. Cortical surface-based analysis. I. Segmentation and surface reconstruction. Neuroimage. 1999;9(2):179-94.
113. Desikan RS, Segonne F, Fischl B, Quinn BT, Dickerson BC, Blacker D, et al. An automated labeling system for subdividing the human cerebral cortex on MRI scans into gyral based regions of interest. Neuroimage. 2006;31(3):968-80.
114. Fischl B, Dale AM. Measuring the thickness of the human cerebral cortex from magnetic resonance images. Proc Natl Acad Sci U S A. 2000;97(20):11050-5.
115. Fischl B, Salat DH, Busa E, Albert M, Dieterich M, Haselgrove C, et al. Whole brain segmentation: automated labeling of neuroanatomical structures in the human brain. Neuron. 2002;33(3):341-55.
116. Fischl B, Sereno MI, Tootell RB, Dale AM. High-resolution intersubject averaging and a coordinate system for the cortical surface. Hum Brain Mapp. 1999;8(4):272-84.
117. Segonne F, Dale AM, Busa E, Glessner M, Salat D, Hahn HK, et al. A hybrid approach to the skull stripping problem in MRI. Neuroimage. 2004;22(3):1060-75.
118. Sled JG, Zijdenbos AP, Evans AC. A nonparametric method for automatic correction of intensity nonuniformity in MRI data. IEEE Trans Med Imaging. 1998;17(1):87-97.
119. Segonne F, Pacheco J, Fischl B. Geometrically accurate topology-correction of cortical surfaces using nonseparating loops. IEEE Trans Med Imaging. 2007;26(4):518-29.
120. Fischl B, Sereno MI, Dale AM. Cortical surface-based analysis. II: Inflation, flattening, and a surface-based coordinate system. Neuroimage. 1999;9(2):195-207.
121. Fischl B, van der Kouwe A, Destrieux C, Halgren E, Segonne F, Salat DH, et al. Automatically parcellating the human cerebral cortex. Cereb Cortex. 2004;14(1):11-22.
122. Rosas HD, Liu AK, Hersch S, Glessner M, Ferrante RJ, Salat DH, et al. Regional and progressive thinning of the cortical ribbon in Huntington's disease. Neurology. 2002;58(5):695-701.

123. Kuperberg GR, Broome MR, McGuire PK, David AS, Eddy M, Ozawa F, et al. Regionally localized thinning of the cerebral cortex in schizophrenia. Arch Gen Psychiatry. 2003;60(9):878-88.
124. Salat DH, Buckner RL, Snyder AZ, Greve DN, Desikan RS, Busa E, et al. Thinning of the cerebral cortex in aging. Cereb Cortex. 2004;14(7):721-30.
125. Han X, Jovicich J, Salat D, van der Kouwe A, Quinn B, Czanner S, et al. Reliability of MRI-derived measurements of human cerebral cortical thickness: the effects of field strength, scanner upgrade and manufacturer. Neuroimage. 2006;32(1):180-94.
126. Ashburner J. A fast diffeomorphic image registration algorithm. Neuroimage. 2007;38(1):95-113.
127. Chao-Gan Y, Yu-Feng Z. DPARSF: A MATLAB Toolbox for "Pipeline" Data Analysis of Resting-State fMRI. Front Syst Neurosci. 2010;4:13.
128. MATLAB 8.0 and Statistics Toolbox 8.1 TM, Inc., Natick, Massachusetts, United States.
129. Satterthwaite TD, Elliott MA, Gerraty RT, Ruparel K, Loughead J, Calkins ME, et al. An improved framework for confound regression and filtering for control of motion artifact in the preprocessing of resting-state functional connectivity data. Neuroimage. 2013;64:240-56.
130. Biswal B, Yetkin FZ, Haughton VM, Hyde JS. Functional connectivity in the motor cortex of resting human brain using echo-planar MRI. Magn Reson Med. 1995;34(4):537-41.
131. Lowe MJ, Mock BJ, Sorenson JA. Functional connectivity in single and multislice echoplanar imaging using resting-state fluctuations. Neuroimage. 1998;7(2):119-32.
132. Tzourio-Mazoyer N, Landeau B, Papathanassiou D, Crivello F, Etard O, Delcroix N, et al. Automated anatomical labeling of activations in SPM using a macroscopic anatomical parcellation of the MNI MRI single-subject brain. Neuroimage. 2002;15(1):273-89.
133. Rubinov M, Sporns O. Complex network measures of brain connectivity: uses and interpretations. Neuroimage. 2010;52(3):1059-69.
134. Chun H, Keles S. Sparse partial least squares for simultaneous dimension reduction and variable selection. Journal of the Royal Statistical Society - Series B. 2009.
135. Chung D, Chun H. An Introduction to the ‘spls ’ Package, Version 1.0 [http://cran.r-project.org/web/packages/spls/vignettes/spls-example.pdf%5D. CiteSeerX; 2010.
136. Kapushesky M, Tikhonov A, Aulchenko YS, Gonçalves A, Rung J, Santamaria R, et al., editors. EBI R CLOUD – Cloud computing for functional genomics at the EBI. URL: http://f1000.com/posters/browse/summary/328. Intelligent Systems for Molecular Biology 2010 meeting; 11 - 13 Jul 2010.
137. Esbensen KH, Guyot D, Westad F, Houmøller LP. Multivariate data analysis in practice: an introduction to multivariate data analysis and experimental design, 5th Edition.: Aalborg University, Esbjerg; 2002.
138. Liaw A, Wiener M. Classification and Regression by randomForest. R News. 2002;2(3):18-22.
139. Cover TM, Thomas JA. Elements of Information Theory, 2nd Edition: Wiley-Interscience; 2006.
140. Breiman L. Random Forests. Machine Learning. 2001;Volume 45, Number 1: 5-32.
141. Max Kuhn. Contributions from Jed Wing SW, Andre Williams, Chris Keefer and Allan Engelhardt. caret: Classification and Regression Training. R package version 5.15-023. http://CRAN.R-project.org/package=caret. 2012.
142. Kuhn M. Vignette: variable selection using the 'caret' package. 2012; Available from: http://cran.cermin.lipi.go.id/web/packages/caret/vignettes/caretSelection.pdf

143. Robin X, Turck N, Hainard A, Tiberti N, Lisacek F, Sanchez J-C, et al. pROC: an open-source package for R and S+ to analyze and compare ROC curves. BMC Bioinformatics, 7, 77. 2011.
144. Yarkoni T, Poldrack RA, Nichols TE, Van Essen DC, Wager TD. Large-scale automated synthesis of human functional neuroimaging data. Nat Methods. 2011;8(8):665-70.
145. Wold S, Ruhe A, Wold H, Dunn WJ, Iii. The Collinearity Problem in Linear Regression. The Partial Least Squares (PLS) Approach to Generalized Inverses. SIAM Journal on Scientific and Statistical Computing. 1984;5:735-43.
146. Westman E, Simmons A, Muehlboeck JS, Mecocci P, Vellas B, Tsolaki M, et al. AddNeuroMed and ADNI: similar patterns of Alzheimer's atrophy and automated MRI classification accuracy in Europe and North America. Neuroimage. 2011;58(3):818-28.
147. Westman E, Muehlboeck JS, Simmons A. Combining MRI and CSF measures for classification of Alzheimer's disease and prediction of mild cognitive impairment conversion. Neuroimage. 2012;62(1):229-38.
148. Weintraub D, Doshi J, Koka D, Davatzikos C, Siderowf AD, Duda JE, et al. Neurodegeneration across stages of cognitive decline in Parkinson disease. Arch Neurol. 2011;68(12):1562-8.
149. Melzer TR, Watts R, MacAskill MR, Pitcher TL, Livingston L, Keenan RJ, et al. Grey matter atrophy in cognitively impaired Parkinson's disease. J Neurol Neurosurg Psychiatry. 2012;83(2):188-94.
150. Gatev P, Darbin O, Wichmann T. Oscillations in the basal ganglia under normal conditions and in movement disorders. Mov Disord. 2006;21(10):1566-77.
151. Hammond C, Bergman H, Brown P. Pathological synchronization in Parkinson's disease: networks, models and treatments. Trends Neurosci. 2007;30(7):357-64.
152. Brown P, Oliviero A, Mazzone P, Insola A, Tonali P, Di Lazzaro V. Dopamine dependency of oscillations between subthalamic nucleus and pallidum in Parkinson's disease. J Neurosci. 2001;21(3):1033-8.
153. Levy R, Ashby P, Hutchison WD, Lang AE, Lozano AM, Dostrovsky JO. Dependence of subthalamic nucleus oscillations on movement and dopamine in Parkinson's disease. Brain. 2002;125(Pt 6):1196-209.
154. Skidmore F, Korenkevych D, Liu Y, He G, Bullmore E, Pardalos PM. Connectivity brain networks based on wavelet correlation analysis in Parkinson fMRI data. Neurosci Lett. 2011;499(1):47-51.
155. Gottlich M, Munte TF, Heldmann M, Kasten M, Hagenah J, Kramer UM. Altered resting state brain networks in Parkinson's disease. PLoS One. 2013;8(10):e77336.
156. Olde Dubbelink KT, Hillebrand A, Stoffers D, Deijen JB, Twisk JW, Stam CJ, et al. Disrupted brain network topology in Parkinson's disease: a longitudinal magnetoencephalography study. Brain. 2013.
157. Mink JW. The basal ganglia: focused selection and inhibition of competing motor programs. Prog Neurobiol. 1996;50(4):381-425.
158. Zgaljardic DJ, Borod JC, Foldi NS, Mattis PJ, Gordon MF, Feigin A, et al. An examination of executive dysfunction associated with frontostriatal circuitry in Parkinson's disease. J Clin Exp Neuropsychol. 2006;28(7):1127-44.
159. Stocco A, Lebiere C, Anderson JR. Conditional routing of information to the cortex: a model of the basal ganglia's role in cognitive coordination. Psychol Rev. 2010;117(2):541-74.
160. Vovk V, Gammerman A, Shafer G. Algorithmic Learning in a Random World: Springer US; 2005.

161. Gammerman A, Vovk V. Hedging Predictions in Machine Learning. The Computer Journal. 2007;50(2):151-63.
162. Nouretdinov I, Lebedev A. Defensive Forecast for Conformal Bounded Regression. In: Papadopoulos H, Andreou A, Iliadis L, Maglogiannis I, editors. Artificial Intelligence Applications and Innovations: Springer Berlin Heidelberg; 2013. p. 384-93.